Regulatory T cells engineered with TCR signaling-responsive IL-2 nanogels suppress alloimmunity in sites of antigen encounter

Eskandari, Siawosh K.; Sulkaj, Ina; Melo, Mariane B.; Li, Na; Allos, Hazim; Alhaddad, Juliano B.; Kollar, Branislav; Borges, Thiago J.; Eskandari, Arach S.; Zinter, Max A.

Published in:
Science Translational Medicine

DOI:
10.1126/scitranslmed.aaw4744

Publication date:
2020

TRANSPLANTATION

Regulatory T cells engineered with TCR signaling–responsive IL-2 nanogels suppress alloimmunity in sites of antigen encounter

Siawosh K. Eskandari[1,2]*, Ina Sulkaj[1,3,4]*, Mariane B. Melo[3,4]*, Na Li[3], Hazim Allos[1], Juliano B. Alhaddad[1], Branislav Kollar[5], Thiago J. Borges[1,6], Arach S. Eskandari[7], Max A. Zinter[8], Songjie Cai[1], Jean Pierre Assaker[1], John Y. Choi[1], Basmah S. Al Dulaijan[1], Amr Mansouri[1], Yousef Haik[1], Bakhos A. Tannous[8], Willem J. van Son[2], Henri G. D. Leuvenink[9], Bohdan Pomahac[5], Leonardo V. Riella[1,6], Li Tang[10,11], Marc A. J. Seelen[2], Darrell J. Irvine[3,4,12,13†], Jamil R. Azzi[1†]

Adoptive cell transfer of ex vivo expanded regulatory T cells (T_{regs}) has shown immense potential in animal models of auto- and alloimmunity. However, the effective translation of such T_{reg} therapies to the clinic has been slow. Because T_{reg} homeostasis is known to require continuous T cell receptor (TCR) ligation and exogenous interleukin-2 (IL-2), some investigators have explored the use of low-dose IL-2 injections to increase endogenous T_{reg} responses. Systemic IL-2 immunotherapy, however, can also lead to the activation of cytotoxic T lymphocytes and natural killer cells, causing adverse therapeutic outcomes. Here, we describe a drug delivery platform, which can be engineered to autostimulate T_{regs} with IL-2 in response to TCR-dependent activation, and thus activate these cells in sites of antigen encounter. To this end, protein nanogels (NGs) were synthesized with cleavable bis(*N*-hydroxysuccinimide) cross-linkers and IL-2/Fc fusion (IL-2) proteins to form particles that release IL-2 under reducing conditions, as found at the surface of T cells receiving stimulation through the TCR. T_{regs} surface-conjugated with IL-2 NGs were found to have preferential, allograft-protective effects relative to unmodified T_{regs} or T_{regs} stimulated with systemic IL-2. We demonstrate that murine and human NG–modified T_{regs} carrying an IL-2 cargo perform better than conventional T_{regs} in suppressing alloimmunity in murine and humanized mouse allotransplantation models. In all, the technology presented in this study has the potential to improve T_{reg} transfer therapy by enabling the regulated spatiotemporal provision of IL-2 to antigen-primed T_{regs}.

INTRODUCTION

Regulatory T cells (T_{regs}) are a subset of helper $CD4^+$ T cells that coexpress the high-affinity interleukin-2 (IL-2) receptor α, CD25, and the transcription factor Forkhead box p3 (Foxp3) (*1*–*3*). As modulators of innate and adaptive immune responses to both foreign and self-antigens, T_{reg} therapies are considered to have numerous clinical applications (*4*, *5*). Despite the slow translation of early preclinical findings, however, recent years have been marked by encouraging efforts to translate T_{reg} immunotherapies to the clinic for preventing acute and chronic graft rejection, graft-versus-host disease (GvHD), and autoimmune diseases such as type 1 diabetes (*6*–*8*). Specifically, in the context of alloimmunity, adoptive T_{reg} therapies tip the immunological scales in favor of immunoregulation by promoting intragraft T_{reg} dominance and attenuating the proinflammatory processes that precipitate graft loss (*9*–*11*).

For therapeutic T_{reg} strategies, peripheral T_{regs} are isolated from the blood of patients, expanded ex vivo, and adoptively transferred back (*12*–*14*). Critical for the success of these therapies is the ex vivo expansion of T_{regs}, because induction of immune tolerance by T_{regs} relies on both the qualitative and quantitative inhibition of proinflammatory cells (*15*). Attaining relevant therapeutic outcomes in a lymphoreplete individual can thus require as many as 50×10^9 polyclonal T_{regs} (*16*), although antigen-specific T_{regs} are known to be more effective in suppressing alloimmunity at lower cell numbers (*17*, *18*). Apart from quantitative impediments, clinical T_{reg} strategies are additionally hampered by qualitative constraints. In particular, the unstable expression of the master T_{reg} regulator, Foxp3, predisposes T_{regs} to convert into proinflammatory counterparts upon in vivo injection (*19*–*22*). To drive T_{reg} expansion, maintain constant Foxp3 expression, and sustain immunosuppressive qualities, T_{regs} require continuous T cell receptor (TCR) ligation (*23*, *24*) and a favorable environment of exogenously produced factors such as IL-2 (*25*–*27*).

The dependence of T_{regs} on IL-2 and its high-affinity receptor CD25 underpinned the discovery of T_{regs} by Sakaguchi *et al.* (*1*). In contrast to conventional $CD4^+$ T cells, T_{regs} are dependent on external sources of IL-2 because they cannot endogenously synthesize it

[1]Transplantation Research Center, Brigham and Women's Hospital, Harvard Medical School, Boston, MA 02115, USA. [2]Division of Nephrology, University Medical Center Groningen, University of Groningen, 9713 GZ Groningen, Netherlands. [3]Koch Institute for Integrative Cancer Research, Massachusetts Institute of Technology, Cambridge, MA 02142, USA. [4]Department of Biological Engineering, Massachusetts Institute of Technology, Cambridge, MA 02142, USA. [5]Division of Plastic Surgery, Brigham and Women's Hospital, Harvard Medical School, Boston, MA 02115, USA. [6]Center for Transplantation Sciences, Massachusetts General Hospital, Harvard Medical School, Charlestown, MA 02129, USA. [7]Department of Electrical Engineering, Delft University of Technology, 2628 CD Delft, Netherlands. [8]Experimental Therapeutics and Molecular Imaging Unit, Department of Neurology, Neuro-Oncology Division, Massachusetts General Hospital, Harvard Medical School, Boston, MA 02129, USA. [9]Department of Surgery, University Medical Center Groningen, University of Groningen, 9713 GZ Groningen, Netherlands. [10]Institute of Bioengineering, École Polytechnique Fédérale de Lausanne, CH-1015 Lausanne, Switzerland. [11]Institute of Materials Science and Engineering, École Polytechnique Fédérale de Lausanne, CH-1015 Lausanne, Switzerland. [12]Ragon Institute of Massachusetts General Hospital, Massachusetts Institute of Technology, Cambridge, MA 02139, USA. [13]Howard Hughes Medical Institute, Chevy Chase, MD 20815, USA.
*These authors contributed equally to this work.
†Corresponding author. Email: djirvine@mit.edu (D.J.I.); jazzi@bwh.harvard.edu (J.R.A.)

(*28*, *29*). Research on the dependence of peripheral T_{regs} on IL-2 recently culminated in a clinically relevant alternative to adoptive T_{reg} transfer. In various auto- and alloimmune disease models, systemic, low-dose IL-2 proved capable of preferentially stimulating T_{regs} over effector T cells, due to the selective enrichment of CD25 on T_{regs} (*30*–*32*). Nevertheless, a crucial caveat to this approach lies in supplying IL-2 to the T_{regs} at the right site and time, because the systemically administered immunomodulator can spark the simultaneous activation of other proinflammatory cells that share surface expression of CD25 (*33*). A recent clinical study on patients with chronic GvHD who were treated with low-dose IL-2, for example, showed synchronous activation of both T_{regs} and natural killer (NK) cells circulating in the peripheral blood of these patients (*34*).

Here, we demonstrate a drug delivery platform that combines the virtues of adoptive T_{reg} transfer and exogenous IL-2 supplementation by spatiotemporally linking IL-2 release to tissue-specific TCR triggering of adoptively transferred T_{regs}. We recently demonstrated a strategy (*35*) to create TCR signaling–responsive "backpacks" that sensitively released IL-15 to tumor-specific $CD8\alpha^+$ T cells by exploiting the increased cell surface reducing potential of antigenically primed, activated T cells (*36*, *37*). Once T cells—including T_{regs}—are mitogenically stimulated, cytoplasmic and cell surface reducing agents are up-regulated to counter the oxidative stresses secondary to cellular proliferation (*35*, *37*–*39*). Presently, we demonstrate the engineering of immunoregulatory $CD4^+Foxp3^+$ T cells with redox-sensitive IL-2 nanoparticles that provide cytokine-mediated survival stimuli to adoptively transferred T_{regs} undergoing alloantigen-TCR–specific activation in antigen-rich areas, such as the allograft and allograft-draining lymph nodes (Fig. 1A). We hypothesized that these membrane-conjugated backpacks would improve the therapeutic outcomes of T_{reg} therapy without the need for genetic engineering and, thus, keep costs low and safety margins high while having realistic

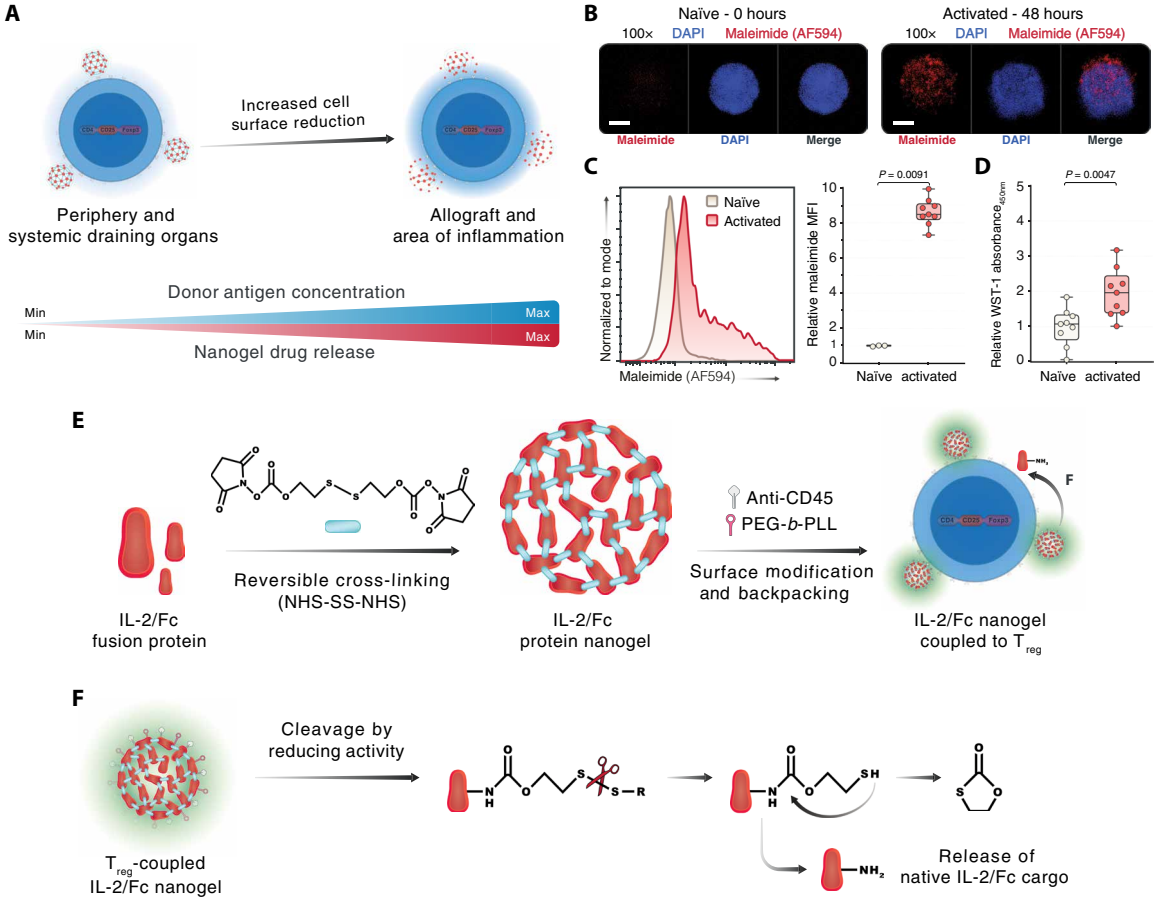

Fig. 1. Designing a TCR signaling–responsive cytokine-delivery platform for T_{regs}. (**A**) Circulating T cells increase their reducing activity in proportion to the donor antigen concentration, which is the highest in areas of inflammation. Nanoparticle backpacks that release their payload in response to a heightened redox potential provide controlled spatiotemporal release of adjuvants. (**B**) Confocal microscopy of free surface thiol staining on naïve T_{regs} versus T_{regs} primed with 4 μg/ml each of soluble anti-CD3ε and anti-CD28 for 48 hours to determine whether T_{regs} up-regulate cell surface redox agents. Scale bars, 5 μm. DAPI, 4′,6-diamidino-2-phenylindole. (**C**) Flow cytometry staining of free surface thiol expression on activated T_{regs} compared with resting, nonactivated T_{regs} among viable $CD4^+$ events ($n = 3$ technical replicates per condition, 3 experiments). MFI, mean fluorescence intensity. (**D**) Colorimetric WST-1 assay on naïve and activated T_{regs} measuring cell surface reductive activity ($n = 3$ technical replicates per condition, 3 experiments). (**E**) Synthesis of reduction-sensitive nanoparticles through reversible cross-linking of IL-2/Fc fusion protein, a survival cytokine for T_{regs}, with bis-NHS cross-linkers, and further surface modification with monoclonal anti-CD45 and PEG-PLL for prolonged surface retention. (**F**) Cleavage of the disulfide bond that maintains the integrity of the backpack, through reducing agents originating from activated T_{regs}, making the native cargo protein, IL-2/Fc, available to the host T_{reg}. Fold changes were normalized against the CT condition. Throughout, data are represented as boxplots with median, interquartile range, minimum, maximum, and all individual data points of the denoted experimental groups. *P* values were calculated with independent samples two-tailed Student's *t* tests, and nonparametric Kolmogorov-Smirnov tests were performed when the assumption of homoscedasticity could not be met.

translational applicability. In our experiments, we found that in addition to the platform foregoing the use of state-of-the-art equipment or techniques and requiring only a simple 45-min incubation step to be conjugated onto T_{regs}, the effects of engineered T_{regs} markedly outlasted those of unmodified T_{regs}.

RESULTS

Functionalizing T_{regs} with a TCR signaling–responsive drug delivery platform

Although we previously demonstrated the efficacy of a redox-sensitive, cytokine-backpacking platform in potentiating effector T cells to curb tumor engraftment (*35*), it was unknown whether T_{regs} could be similarly functionalized to suppress alloimmunity. First, we examined whether T_{regs} increase their free surface thiol expression and reducing activity upon TCR ligation. We found that $CD4^+CD25^+$ T_{regs} magnetically sorted from C57BL/6 murine splenocytes and stimulated for 48 hours with monoclonal antibodies (mAbs) against CD3ε and CD28 increased the expression of unbound surface thiols by confocal microscopy (Fig. 1B). In parallel, using flow cytometry, we observed an increase in the free surface thiol expression on activated T_{regs} versus naïve T_{regs} (Fig. 1C and fig. S1A), similar to the increase in $CD4^+$ and $CD8\alpha^+$ T cells upon CD3/CD28-mediated stimulation (fig. S1, B to D). Last, we confirmed the increased reducing activity at the surface of activated T_{regs} using colorimetric water-soluble tetrazolium (WST)-1 assays, which measure the conversion of the stable WST-1 salt into the fluorescent formazan. This conversion is driven by reducing agents that are secreted from metabolically active cells, thus gauging the activation state of cells through their redox potential. In these WST-1 assays, we delineated a ~2-fold increase in the redox potential of activated T_{regs} compared with naïve T_{regs} (Fig. 1D). Building on these findings, we used disulfide-containing bis(*N*-hydroxysuccinimide) (bis-NHS) cross-linkers, which are redox sensitive, to weave together cytokine or protein cargo as adducted prodrugs in the form of nanoscale gels [nanogels (NGs)]. Conjugating these redox-sensitive NGs onto T_{regs} would then allow for the release of the native cargo upon cleavage of the self-immolative linkers (*40*, *41*). To understand whether redox-responsive NGs made from IL-2 could autostimulate and stabilize T_{regs}, we synthesized IL-2/Fc NGs. The rationale behind using IL-2/Fc over wild-type IL-2 was its improved stability and half-life compared to the latter, allowing for longer-lasting in vitro and in vivo effects. In addition, we included a single amino acid mutation (D265A) in the Fc sequence to prevent the deposition of complement and the formation of humoral immunity against the Fc portion (*42*). We focused our efforts on IL-2 in particular because its roles in promoting T_{reg} homeostasis and stability are well established (*25*–*27*). In addition, to promote the stable anchoring of the NGs onto the T_{reg} surface and to prevent the premature internalization of the NGs, we further surface-modified the NGs with monoclonal anti-CD45 and polyethylene glycol–*b*-poly(*L*-lysine) (PEG-PLL) (Fig. 1E). We previously showed that binding NGs to the surface of T cells through CD45 provides a noninternalizing surface anchor expressed exclusively on leukocytes and CD45 ligation in itself does not affect T cell proliferation (*35*, *43*, *44*). The cleavage of the integral disulfide bond in the NG cross-linkers is ultimately driven by the increased reducing activity at the surface of activated T_{regs}, thus releasing the native IL-2/Fc cargo for autocrine capture by cell surface CD25 and subsequent CD25-mediated survival signaling (Fig. 1F).

Surface engineering of T_{regs} with IL-2/Fc NG does not alter T_{reg} phenotype

Next, we examined whether IL-2/Fc NGs could be conjugated to T_{regs} and whether this conjugation would affect the T_{reg} phenotype. Using flow cytometry (fig. S1A), we found that incubating magnetically isolated T_{regs} with fluorophore-labeled, anti-CD45–bearing IL-2/Fc NGs at 4°C for 45 min did not reduce the coexpression of CD25 and Foxp3 among $CD4^+$ T cells compared with control (CT) T_{regs} (Fig. 2A). Among the T_{regs} that were incubated with IL-2/Fc NGs, however, >90% acquired fluorescein isothiocyanate (FITC) fluorescence, indicating successful membrane conjugation of the NGs (Fig. 2, B to D, and movies S1 and S2). In in vitro release assays, we then found that the release of IL-2/Fc from NGs was driven by glutathione (GSH; a reducing agent), with ~90% of the cross-linked IL-2/Fc being released within 6 days in the presence of GSH (fig. S2A). We additionally studied the duration of IL-2/Fc NG retention on the surface of NG-coupled T_{regs} stimulated in vitro for 3 and 7 days with anti-CD3ε and anti-CD28 to appraise the degree of NG dilution on the T_{reg} surface with mitosis. Using flow cytometry, we found that ~30 and ~20% of T_{regs} cultured in the presence of anti-CD3ε/CD28 for 3 and 7 days, respectively, retained surface expression of IL-2/Fc NGs (fig. S2B). Although, expectedly, most of the NG-engineered T_{regs} lost surface expression of the NGs after activation, the cells that maintained NG expression retained phenotypic markers related to T_{reg} functionality, namely, CD25 and cytotoxic T-lymphocyte-associated protein (CTLA)-4. In contrast, T_{regs} that lost NG surface expression down-regulated the same markers (fig. S2, C and D).

To delineate the effects of IL-2/Fc NGs on T_{reg} survival, we studied T_{reg} survival among unmodified, untouched T_{regs} (CT), T_{regs} receiving soluble IL-2/Fc stimulation (CT + IL-2/Fc), and NG-conjugated T_{regs} (NG) in in vitro stimulation assays. In these experiments, all T_{reg} conditions were cultured for 3 and 7 days with a constant concentration of anti-CD28 and titrated concentrations of anti-CD3ε to appraise the relation between TCR signaling strength and NG-dependent survival outcomes. We postulated that the redox-sensitive IL-2/Fc NGs would release IL-2/Fc under reducing conditions at the T_{reg} surface, which would be contingent on the CD3 dose-dependent activation of T_{regs} and, thus, selectively promote pro-survival effects at higher CD3ε concentrations. To characterize the survival outcomes, we compared the maintenance of the $CD4^+CD25^+Foxp3^+$ phenotype, the absolute counts of T_{regs}, and the mean expression of surface-expressed coinhibitory and stimulatory glycoproteins tied to T_{reg} function (*45*–*49*). At day 3 after stimulation and across all concentrations of anti-CD3ε, T_{regs} cultured with free IL-2/Fc and IL-2/Fc NGs maintained a higher expression of CD25 and Foxp3 compared to the untouched CT T_{regs}, without the off-target proliferation of non-$CD4^+$ T cells (Fig. 2E and fig. S3, A to C). In addition, the percentages and absolute counts of $CD4^+CD25^{hi}Foxp3^+$ T_{regs} were higher for the CT + IL-2/Fc and NG conditions compared to the CT condition (Fig. 2F). Only at the highest concentration of anti-CD3ε, however, there were >25- and >50-fold $CD25^{hi}Foxp3^+$ T_{regs} under the CT + IL-2/Fc and NG conditions, respectively, compared to the CT condition. At day 7 after stimulation, there were similar CD3-dependent increases in the absolute counts of $CD25^{hi}Foxp3^+$ T_{regs} under the CT + IL-2/Fc and NG conditions but, again, without discernible CD3-dependent effects among the CT T_{regs} (Fig. 2, G to H, and fig. S3, D and E). In addition, at the highest concentration of anti-CD3ε, there were >10- and >11-fold $CD25^{hi}Foxp3^+$ T_{regs} under the CT + IL-2/Fc and NG

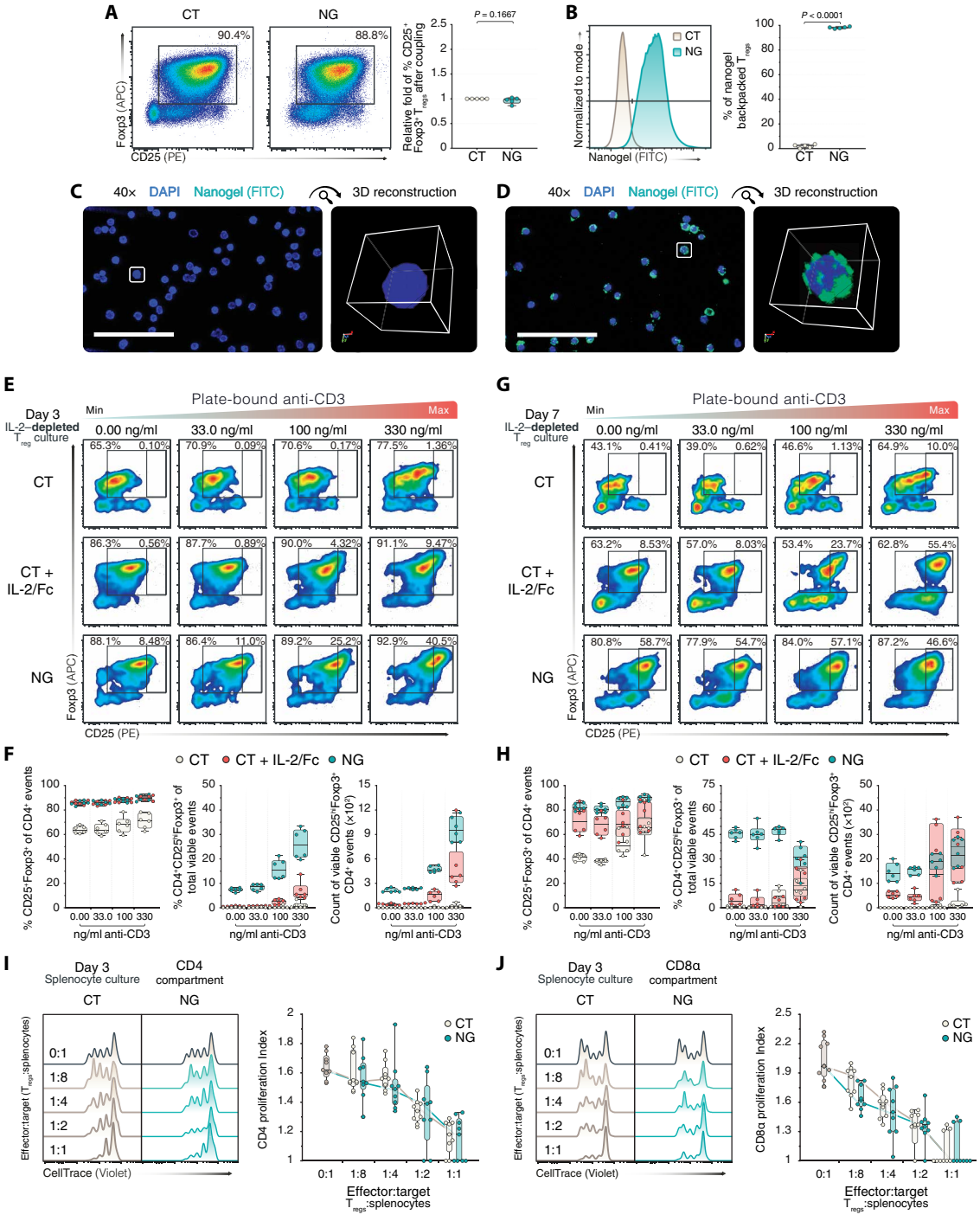

Fig. 2. Surface engineering of T_{regs} with IL-2/Fc NG does not alter T_{reg} phenotype. (**A** and **B**) Coexpression of CD25 and Foxp3 among $CD4^+$ T cells (A) and the expression of FITC-labeled NGs on these $CD4^+CD25^+Foxp3^+$ cells (B) comparing control, unmodified T_{regs} (CT), and IL-2/Fc NG-conjugated T_{regs} (NG; $n = 5$ experiments). PE, phycoerythrin. (**C** and **D**) Confocal microscopy images of CT (C) and NG (D) T_{regs}. Scale bars, 100 μm. (**E**) Flow cytometric analysis of CT T_{regs}, CT T_{regs} cultured with soluble IL-2/Fc (CT + IL-2/Fc), and NG T_{regs} stimulated in vitro with plate-bound anti-CD28 (1 μg/ml) and titrated concentrations (0 to 330 ng/ml) of plate-bound anti-CD3ε for 3 days, assaying $CD25^+Foxp3^+$ percentages among $CD4^+$ T cells. (**F**) Box plots of $CD25^+Foxp3^+$ percentages among $CD4^+$ events, $CD4^+CD25^{hi}$ $Foxp3^+$ percentages among all live events, and counts of total live $CD4^+CD25^{hi}Foxp3^+$ events ($n = 3$ technical replicates per condition, 2 experiments, *P* values provided in data file S1). (**G** and **H**) Flow cytometric analysis of CT, CT + IL-2/Fc, and NG T_{regs} cultured for 7 days (G) and assayed across the same metrics as described in (E) and (F) (H) ($n = 3$ technical replicates per condition, 2 experiments, *P* values provided in data file S1). (**I** and **J**) Dye dilution suppression assays with suppressor T_{regs} and CellTrace Violet–labeled effector splenocytes in the presence of 4 μg/ml each of soluble anti-CD3ε and anti-CD28, assessing the $CD4^+$ (I) and $CD8\alpha^+$ (J) compartments, respectively ($n = 3$ technical replicates per condition, 3 experiments). All fold changes were normalized against the CT condition. Throughout, data are represented as boxplots with median, interquartile range, minimum, maximum, and all individual data points of the denoted experimental groups. *P* values were calculated with independent samples two-tailed Student's *t* tests, and nonparametric Kolmogorov-Smirnov tests were performed when the assumption of homoscedasticity could not be met. For experimental groups with matched data points across multiple time points or concentrations, mixed-effects model analyses with the Geisser-Greenhouse correction were performed, followed by Holm-Šídák multiple comparison tests.

conditions, respectively, compared to the CT condition, with fewer phenotype-positive T_{regs} at lower anti-CD3ε concentrations for the CT + IL-2/Fc and NG T_{regs} compared with the highest anti-CD3ε concentration.

Next, we assessed whether IL-2/Fc from the NG T_{regs} could stimulate neighboring effector T cells. At sites of immune activation, predominantly in the draining lymph nodes and allografts, T_{regs} are often mingled with conventional CD8 T cells that are also IL-2

responsive (*50*). Patients who are given T_{reg}-tailored IL-2 therapy specifically receive low-dose injections to prevent the off-target activation of proinflammatory CD8 T cells, which can undermine desired immunosuppression end goals (*31*, *50*). Therefore, we appraised the possible IL-2 responsiveness of CD8α$^+$ T cells to IL-2/Fc NGs by coculturing CT, CT + IL-2/Fc, and NG T_{regs} with magnetically sorted CD8α$^+$ T cells in a ratio of 1:5 T_{regs}-to-CD8 T cells and stimulated the cells with anti-CD3ε/CD28 for 3 and 24 hours. A physiological ratio of T_{regs}-to-CD8 T cells was chosen to obviate the natural suppression of the CD8α$^+$ T cells by the T_{regs} and thus maintain a balance between the suppressive effects of the T_{regs}, T_{reg} homeostasis, and CD8 homeostasis. IL-2–mediated signaling in T_{regs} and CD8α$^+$ T cells was assessed through flow cytometric analysis (fig. S3F) of phosphorylated signal transducer and activator of transcription 5 (pSTAT5), which is the key transcription factor actuated by IL-2 receptor signaling (*51*). Within 24 hours, in the NG coculture samples, despite the presence of IL-2/Fc backpacks on the T_{regs}, we observed no discernible pSTAT5 among the CD8α$^+$ T cells, contrasted by most of the T_{regs} being pSTAT5$^+$ (fig. S3, G and H). Compared with the NG coculture samples, however, a subset of the CT + IL-2/Fc CD8α$^+$ T cells showed a distinct increase in pSTAT5 at the 24-hour time point. The latter suggests that IL-2/Fc released from backpacked NG T_{regs} is consumed by the high-affinity IL-2 receptor, CD25, before it can spill over to neighboring CD8α$^+$ T cells, whereas IL-2/Fc access and subsequent IL-2–mediated signaling are more equivalent for the T_{regs} and the CD8α$^+$ T cells in the CT + IL-2/Fc coculture samples.

In addition, for the in vitro cultured T_{regs}, we mapped the T_{reg} phenotype by studying the mean expressions of programmed cell death protein (PD)-1, CTLA-4, and lymphocyte-activation gene (LAG)-3, which are coinhibitory molecules known to be essential for T_{reg} suppressive function (*45*–*48*), and CD69, which is a general marker of lymphocytic activation including T_{regs} (*49*). At day 3 after stimulation, we observed no CD3 dose-dependent effects on the expression of the coinhibitory or activation-induced markers on CT T_{regs} (fig. S3, I to M). In the same time frame, however, we found that NG T_{regs} expressed higher concentrations of these markers compared to CT and CT + IL-2/Fc T_{regs}, whereas CT + IL-2/Fc T_{regs} also showed higher expression of these markers compared to CT T_{regs}. At day 7 after stimulation, the results were similar in showing higher, CD3 dose-dependent expression of the coinhibitory and activation-induced markers on NG and CT + IL-2/Fc T_{regs} compared to the CT T_{regs} (fig. S3, N to R).

Last, to assess the functionality of NG-coupled T_{regs} and to rule out a decrease in their suppressive function, we used an in vitro dye dilution assay. We isolated murine splenocytes as target cells and stained them with a trace dye to track the number of divisions of these splenocytes in culture. We then cocultured these target cells for 3 days with either unmodified, untouched CT T_{regs}, or NG T_{regs} (both freshly isolated) in the presence of anti-CD3ε/CD28 mAbs, culturing a fixed number of target splenocytes with increasing numbers of effector T_{regs}. Upon assessing the target CD4$^+$ and CD8α$^+$ T cell compartments of the cultured splenocytes, we observed a similar dose-dependent suppression of the splenic T cells by both CT and NG T_{regs} ($R > 0.900$, $P < 0.001$) (Fig. 2, I and J, and fig. S4).

NG-engineered T_{regs} suppress in vivo alloimmunity better than conventional T_{regs}

After exploring the in vitro effects of IL-2/Fc NGs on T_{reg} homeostasis, we evaluated the in vivo suppressive function of NG T_{regs} in a murine allotransplantation model. Opting for a stringent, fully major histocompatibility complex (MHC)–mismatched skin transplant model, we grafted BALB/c skin allografts onto the dorsal trunks of immunodeficient recombination-activating gene (*Rag*)$1^{-/-}$ mice on a C57BL/6 (B6) background. Three days later, we intravenously injected equal numbers of immunogenic B6 CD8α$^+$ T cells that drive the rejection process and immunoregulatory B6 CD4$^+$CD25$^+$ T_{regs}, either modified with IL-2/Fc NGs (NG) or unmodified control T_{regs} (CT), which mitigate the alloimmune cascades (Fig. 3A). In light of recent studies that established the validity of systemic IL-2 therapy (*30*–*32*), we also administered soluble IL-2/Fc with CT T_{regs} under a separate condition (CT + IL-2/Fc). The IL-2/Fc concentration injected per mouse under this condition was dosed equivalent to the IL-2/Fc released from the transferred NG T_{regs} per mouse (more details provided in Materials and Methods). Seven days after the adoptive T cell transfer, we analyzed the nondraining lymph nodes and spleens (distal to the site of alloimmunity) and the draining lymph nodes and skin allografts (proximal to the site of alloimmunity) (Fig. 3B), based on our hypothesis that NG T_{regs} would proliferate better than conventional T_{regs} within the alloimmune microenvironment.

Histological analysis of the allografts of the CT- and CT + IL-2/Fc–treated conditions 7 days after the adoptive T_{reg} transfer showed signs of epidermal thickening and perivascular lymphocytic infiltrates, compared to naïve, untransplanted BALB/c skin. T cell infiltration under these conditions was then gauged by immunofluorescence staining for CD3ε, the T cell co-receptor expressed on both CD4$^+$ and CD8α$^+$ T cells, showing greater CD3ε$^+$ infiltrates under the CT and CT + IL-2/Fc conditions (Fig. 3C). In addition, in these groups, there was a disruption of the adnexal structures and the native skin architecture, which are in line with high grades of rejection. The skin grafts of NG-treated mice, on the contrary, showed rare lymphocytic infiltrates, had mild signs of inflammation in the overlying epidermis, and had intact adnexal structures (for example, the hair follicles). Macroscopic examination of the skin showed attenuated signs of allograft rejection in the NG-treated mice compared to CT- and CT + IL-2/Fc–treated mice by day 7 after adoptive transfer, with ~70% of the NG grafts looking healthy compared to ~40% of the CT and ~30% of the CT + IL-2/Fc grafts (Fig. 3D).

Using flow cytometry (fig. S5), we then assayed the percentages of CD4$^+$CD25$^+$Foxp3$^+$ T_{regs} and CD8α$^+$ T cells within the distally and proximally draining tissue sites, as well as the ratio of T_{regs} to CD8α T cells in each draining site, normalizing the fold changes of the T_{reg}-to-CD8 ratios against the CT condition. We observed that systemic IL-2/Fc increased T_{reg} percentages and decreased CD8α$^+$ percentages in the spleen (Fig. 3, E and F, fig. S6A and B), which resulted in increased T_{reg}-to-CD8α ratios in the spleen (Fig. 3G). The systemic IL-2/Fc, however, provided limited advantages over lone CT T_{reg} transfer in the allograft-draining lymph nodes and the allograft in terms of the T_{reg}-to-CD8α ratio. NG treatment, in contrast, precipitated no increase in the T_{reg}-to-CD8α ratios in the distal lymph nodes and spleens. The NG treatment did, however, show an increase in T_{reg}-to-CD8α ratios in the graft-draining lymph nodes and allografts, which constitute the proximal sites of alloimmunity. Several other observations supported the histological and phenotypic findings that NG-treated mice had healthier allografts, including the increased allograft sizes among NG-treated mice (Fig. 3H). Moreover, splenocytes isolated from the different groups (CT, CT + IL-2/Fc, and NG) were stimulated ex vivo for 48 hours with irradiated naïve donor BALB/c splenocytes to test for alloimmune

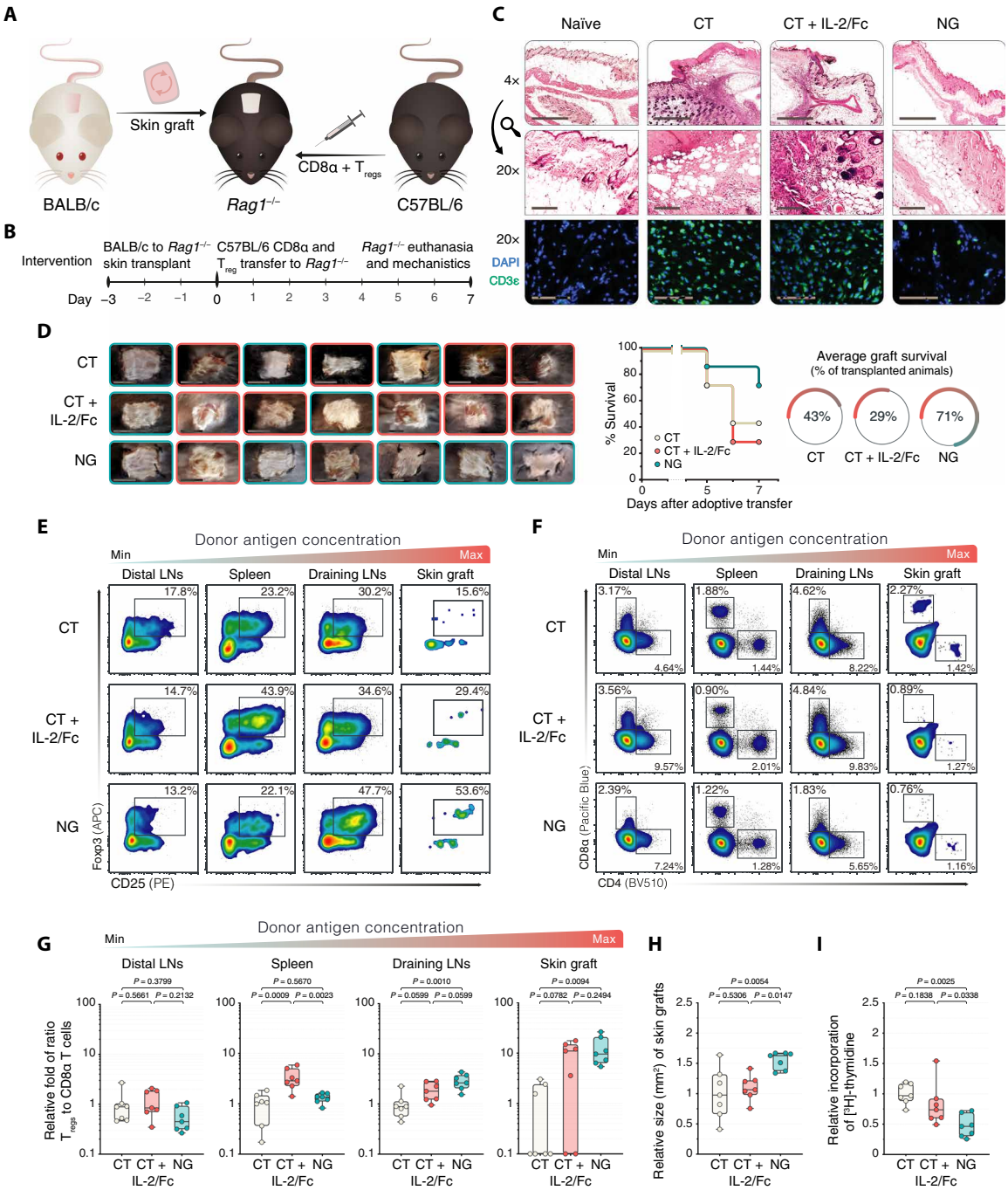

Fig. 3. NG-engineered T_{regs} suppress in vivo alloimmunity better than conventional T_{regs}. *Rag1*$^{-/-}$ mice on a C57BL/6 background were transplanted with fully MHC-mismatched BALB/c allografts 3 days before the adoptive transfer of 5.0×10^5 C57BL/6 CD8α^+ cells and 5.0×10^5 C57BL/6 T_{regs}, with or without IL-2/Fc NG. In addition, a group of control mice was treated with CD8α^+ cells, T_{regs}, and systemic IL-2/Fc. On day 7, the mice were euthanized, and various tissues were analyzed by histology, immunofluorescence, and flow cytometry ($n = 7$ biological replicates per condition, 2 experiments). (**A** and **B**) Experimental mouse model (A) and time line (B). (**C**) Hematoxylin and eosin (H&E) and CD3ε immunofluorescence staining of the experimental conditions and naïve, untreated *Rag1*$^{-/-}$ skin. Scale bars, 1.00 mm (4× H&E), 150 μm (20× H&E), and 100 μm (20× immunofluorescence). (**D**) Macroscopic images of each murine replicate's allograft for all three treatment conditions at the experimental end point with red box borders indicating rejection, complemented with the survival curves and percentages at day 7. Scale bars, 10.0 mm. (**E** and **F**) Flow cytometric analyses of CD25$^+$Foxp3$^+$ T_{regs} among viable CD4$^+$ events (E) and CD8α^+ T cells among viable events (F) across the four distal-to-proximal tissue compartments for CT-, CT + IL-2/Fc–, and NG-treated mice. (**G**) Fold changes of the T_{reg}-to-CD8α ratios in the distal-to-proximal draining sites. (**H**) Fold changes of the skin allograft surface areas. (**I**) Fold changes of the [^{3}H]-thymidine incorporation in mixed lymphocyte reactions of host *Rag1*$^{-/-}$ splenocytes with irradiated donor BALB/c splenocytes. All fold changes were normalized against the CT condition. Throughout, data are represented as boxplots with median, interquartile range, minimum, maximum, and all individual data points of the denoted experimental groups. *P* values were calculated with one-way analyses of variance followed by Holm-Šídák multiple comparison tests. LNs, lymph nodes.

memory responses. After 48 hours, the cocultured splenocytes were pulsed for another 12 to 16 hours in the presence of [methyl-^{3}H]-thymidine to measure alloantigen-specific cell proliferation. We observed that, compared with the CT- and CT + IL-2/Fc–treated conditions, there was a reduction (>2-fold) of alloimmune memory proliferation among the host splenocytes of NG-treated mice (Fig. 3I).

Last, clinical studies using systemic IL-2 injections as a tolerogenic T_{reg}-centric therapy have shown that systemic IL-2 treatment not only stimulates T_{regs} but can also induce off-target expansion of NK cells (*33*, *34*), among other proinflammatory cells. To ensure that our IL-2/Fc NGs delivered IL-2/Fc specifically to T_{regs}, we additionally assessed the effects of the IL-2/Fc NGs on the endogenously present NK compartment in our transplanted *Rag1*$^{-/-}$ mice (fig. S6C). Despite no discernible increases in the percentages of NK cells across all distal-to-proximal tissue sites, we observed lower absolute counts of NK cells in the draining lymph nodes of the NG T_{reg}–treated mice compared with the CT T_{reg}– and CT + IL-2/Fc T_{reg}–treated mice, suggesting the selective release of IL-2/Fc to the T_{regs} in the NG T_{reg}–treated mice compared to the other conditions (fig. S6, D and E).

NG-engineered T_{regs} prolong murine allograft survival better than conventional T_{regs}

Next, we compared the therapeutic effects of conventional T_{regs}, T_{regs} supplemented with systemic IL-2/Fc and NG-engineered T_{regs} by transplanting new groups of *Rag1*$^{-/-}$ mice using the same mismatched BALB/c to B6 allotransplant model as described earlier (Fig. 4, A and B). Whereas the mean survival time of the allotransplants for both CT- and CT + IL-2/Fc–treated conditions was 6 days after adoptive transfer, the allograft survival of mice treated with 10 μg of IL-2/Fc NG/10^6 T_{regs} was lengthened to 10-day mean survival time after adoptive transfer (Fig. 4C). By increasing the surface-conjugated dose of IL-2/Fc NG to 20 μg/10^6 T_{regs}, we observed a further prolongation of the allograft survival to 18 days after adoptive transfer, effectively increasing allograft survival threefold compared with the CT-treated mice (Fig. 4C).

These improved mechanistic and survival results for NG-engineered T_{regs} highlight the functional differences between unmodified CT and NG T_{regs}. However, these results did not allow us to visualize the T_{regs} and CD8 T cells in vivo to understand the local impact of IL-2/Fc NGs on T_{reg} homeostasis and the suppression of alloimmunity. To answer this question, we developed a dual imaging T cell tracking assay to follow the T_{reg} and CD8 T cell populations in vivo. Using retroviral vectors, we transduced two separate bioluminescent luciferase reporters encoding for *Gaussia* luciferase (GLuc) and *Cypridina* luciferase (CLuc; fig. S7A) into preactivated T_{regs} and CD8α$^+$ T cells, respectively (fig. S7, B and C). Because each luciferase can only catalyze the conversion of its own substrate, we could monitor one luciferase without affecting the other luciferase in the same biological sample (fig. S7, D to G). After the T cell transductions, we transferred 5.0×10^5 CD8α-CLuc cells and T_{reg}-GLuc cells each (with or without IL-2/Fc NGs) into *Rag1*$^{-/-}$ mice that were transplanted with BALB/c skin 3 days prior (Fig. 4D). Seven days after the adoptive T cell transfer, we gauged the in vivo bioluminescent signal intensities for GLuc and CLuc. We observed that NG-engineered T_{regs} expressing GLuc colocalized more readily within the skin grafts of the transplanted mice compared to the GLuc-transduced CT T_{regs}, which remained predominantly within the spleens (Fig. 4E). In addition, we observed that the allograft infiltration of CD8α$^+$ T cells, as measured by the CLuc signal, was higher for CT-treated mice compared with NG-treated mice (Fig. 4F). Furthermore, the ratio of T_{reg}-GLuc signals arising from the skin grafts to the T_{reg}-GLuc signals from the whole animals was higher for the NG-treated mice compared to the CT-treated mice, and, similarly, the ratio of the T_{reg}-GLuc signal to CD8α-CLuc signal was higher for NG-treated mice compared to CT-treated mice (Fig. 4G).

Last, we investigated whether the NG platform was promoting activated, antigen-specific T_{regs} in sites of alloimmunity or, instead, the IL-2 release from the NGs was antigen agnostic and milieu dependent. For this question, we compared the effects of CT T_{regs} and NG T_{regs} in an ovalbumin (OVA)–OT-1–OT-2 skin allotransplantation model. We transplanted skin grafts with ubiquitous OVA expression onto the dorsal trunks of immunodeficient *Rag1*$^{-/-}$ mice 3 days before the adoptive transfer of a 2:1:1 ratio of OT-1 CD8α$^+$ T cells, OT-1 CD4$^+$CD25$^+$ T_{regs}, and OT-2 CD4$^+$CD25$^+$ T_{regs} (with or without IL-2/Fc NG; Fig. 4H). The model allowed us to study the role of the NG platform in the homeostasis of nonspecific OT-1 T_{regs} compared to antigen-specific OT-2 T_{regs}. The CD4$^+$ T cells from OT-2 mice can undergo $OVA_{323–339}$–specific clonal expansion through MHC II–dependent presentation of $OVA_{323–339}$ peptides, whereas the CD4$^+$ T cells from OT-1 mice cannot. Thus, because of the nonspecificity of OT-1 CD4$^+$CD25$^+$ T_{regs} for the relevant MHC II–presented OVA peptides, these T_{regs} can only become activated because of environmental stimuli such as cytokines secreted in sites of antigen encounter. OT-2 CD4$^+$CD25$^+$ T_{regs}, on the contrary, will primarily be activated by the $OVA_{323–339}$ peptides. Then, to be able to distinguish the OT-1 cells from the OT-2 cells by flow cytometry, we used a fluorescent tetrameric OT-1 antibody that was specific for the SIINFEKL peptide. Because the *Rag1*$^{-/-}$ hosts lack endogenous T and B cells, the T cells negative for OT-1 were considered to be the remaining adoptively transferred CD4$^+$ T cells, which were the T_{regs} from the OT-2 mice. However, note that in the absence of prior OVA sensitization in the OT-2 mice, a subset of polyclonal T_{regs} with low to negligible OT-2 receptors can be included in the OT-1 tetramer-negative pool of the adoptively transferred OT-2 T_{regs}. Thus, when OT-2 T_{regs} are referenced, the potential inclusion of polyclonal T_{regs} should be factored in, especially in the spleen and nondraining lymph nodes where the exposure to the OT-2–specific $OVA_{323–339}$ peptide is sparser compared with the higher concentrations of $OVA_{323-339}$ in the draining lymph nodes and skin allografts. Seven days after the adoptive T cell transfer, we euthanized the mice and analyzed various distal-to-proximal tissues as described before (Fig. 4I). Using flow cytometry (fig. S8), we determined the percentages of CD4$^+$Foxp3$^+$OT-2$^+$ T_{regs} and OT-1$^+$CD8α$^+$ T cells within the distally and proximally draining tissue sites, as well as the ratio of OT-2 T_{regs} to OT-1 CD8α T cells in each tissue site. Comparing the ratios of OT-2 T_{regs} to OT-1 CD8α T cells across all four compartments, we observed the highest increase in the ratio of OT-2 T_{regs} to OT-1 CD8α of as much as 150-fold and on average 35-fold in the skin allografts of the NG-treated mice compared with the CT-treated mice (Fig. 4J). To understand which T_{reg} responses were dominant in each draining site, that is, nonspecific OT-1 T_{regs} versus antigen-specific OT-2 T_{regs}, we assessed the percentage of OT-1$^+$ versus OT-2$^+$ CD4$^+$Foxp3$^+$ T_{regs}. We found that the dominant T_{reg} type for both CT- and NG-treated mice in all draining sites was the antigen-specific OT-2 T_{reg}. The percentage of OT-2 T_{regs} out of the total T_{regs} (OT-1 + OT-2) in the draining lymph nodes and skin allografts, however, was higher for NG-treated mice compared to

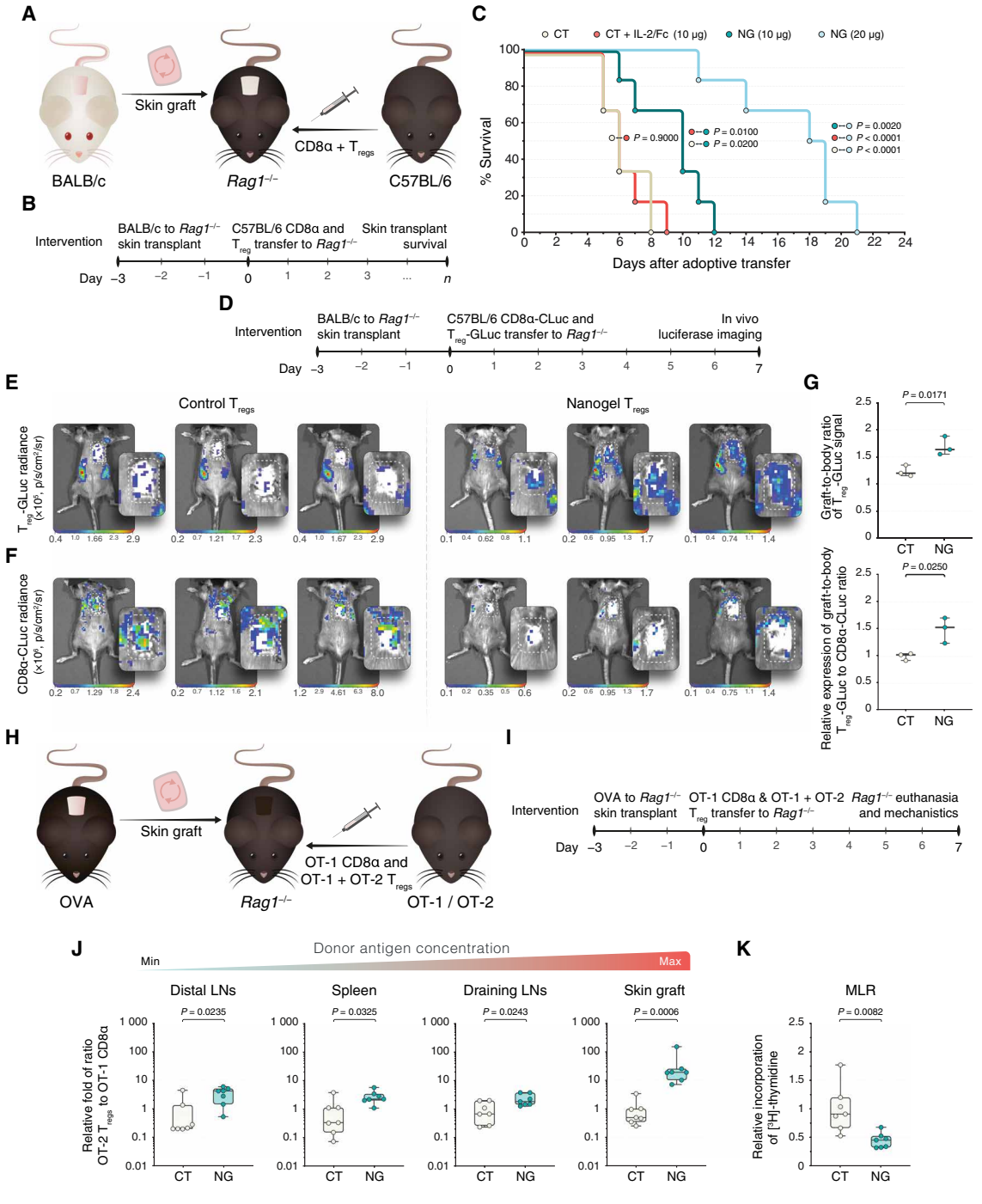

Fig. 4. NG-engineered T_{regs} prolong murine allograft survival better than conventional T_{regs} and differentially promote antigen-specific T_{regs}. Allograft survival was studied using the same *Rag1*$^{-/-}$ to BALB/c model as described in Fig. 3, adoptively transferring 5.0×10^5 C57BL/6 CD8α$^+$ cells and 5.0×10^5 C57BL/6 T_{regs} on day 3 after transplant, without IL-2/Fc NG, with systemic IL-2/Fc, or with IL-2/Fc NG ($n = 6$ mice per group). (**A** and **B**) Experimental mouse survival model (A) and time line (B). (**C**) Survival curves of each of the treatment groups. (**D** to **G**) In vivo T cell responses were tracked by transplanting BALB/c skin grafts onto *Rag1*$^{-/-}$ mice and adoptively transferring 5.0×10^5 C57BL/6 CD8α$^+$ cells transduced with *Cypridina* luciferase (CLuc) and 5.0×10^5 C57BL/6 T_{regs} transduced with *Gaussia* luciferase (GLuc), either unmodified or decorated with IL-2/Fc NGs, on day 3 after transplant ($n = 3$ biological replicates per condition, 1 representative experiment). (D) Experimental bioluminescent T cell tracking model and time line. (E) In vivo imaging of CT and NG T_{reg} GLuc signals after intravenous coelenterazine administration. (F) In vivo imaging of CD8α$^+$ T cell CLuc signals after intravenous *Cypridina* luciferin administration. (G) Ratios of T_{reg}-GLuc signal in the skin grafts compared with the whole animals, and fold changes of T_{reg}-to-CD8α (GLuc-to-CLuc) signal in the skin grafts compared with the whole animals. Last, antigen-specific alloimmunity was assessed with an OVA–OT-1–OT-2 model. *Rag1*$^{-/-}$ mice were transplanted with OVA allografts 3 days before the adoptive transfer of 5.0×10^5 OT-1 CD8α$^+$ T cells, 2.5×10^5 OT-1 CD4$^+$CD25$^+$ T_{regs}, and 2.5×10^5 OT-2 CD4$^+$CD25$^+$ T_{regs}, left untouched or coupled IL-2/Fc NGs. On day 7, the mice were euthanized, and various tissues were analyzed by flow cytometry ($n = 7$ biological replicates per condition, 2 experiments). (**H** and **I**) Antigen-specific mouse model (H) and time line (I). (**J**) Fold changes of the ratio of OT-2 T_{regs} to OT-1 CD8α in the distal-to-proximal draining sites. (**K**) Fold changes of the [^{3}H]-thymidine incorporation in mixed lymphocyte reactions of host *Rag1*$^{-/-}$ splenocytes with irradiated donor OVA splenocytes. All fold changes were normalized against the CT condition. Throughout, data are represented as boxplots with median, interquartile range, minimum, maximum, and all individual data points of the denoted experimental groups. *P* values were calculated with log-rank Mantel-Cox tests, or with independent samples two-tailed Student's *t* tests, and nonparametric Kolmogorov-Smirnov tests were performed when the assumption of homoscedasticity could not be met. MLR, mixed lymphocyte reaction.

CT-treated mice, suggesting that the IL-2/Fc NGs promoted the homeostasis of antigen-specific T_{regs} more efficiently in these proximal draining sites compared to untreated antigen-specific CT T_{regs} (fig. S9A). Furthermore, NG-treated mice had lower counts of antigen-specific OT-1 $CD8\alpha^+$ T cells across all draining sites (fig. S9B). In addition, splenocytes isolated from the two treatment groups (CT and NG) were stimulated ex vivo for 48 hours with irradiated naïve donor OVA splenocytes to test for alloimmune memory responses. This assay showed attenuated memory responses (>2-fold) in the NG-treated mice versus the CT-treated mice (Fig. 4K).

IL-2/Fc NGs conjugated to human T_{regs} improve their function and homeostasis in vitro and in vivo and promote intragraft T_{regs}

Ultimately, we tested the ability of IL-2/Fc NGs to promote human T_{reg} homeostasis in vitro and in vivo. For the in vitro experiments, magnetically sorted human $CD4^+CD25^{hi}CD127^{lo}$ T_{regs} were either left untouched (CT) or coupled with anti-human CD45 IL-2/Fc NGs (NG). The T_{regs} were then stimulated with mAbs against CD3ε/CD28 and analyzed by flow cytometry (fig. S10A) 3 and 7 days after stimulation. Compared with the human CT T_{regs}, the NG T_{regs} had >2- and >5-fold absolute counts of $CD4^+CD25^+CD127^{lo}Foxp3^+$ T cells within 3 days (fig. S10B) and 7 days (fig. S10C), respectively. Building on these in vitro findings, we opted for a preclinical humanized mouse model in which we grafted discarded healthy donor skin from patients undergoing cosmetic surgery onto the dorsal trunks of nonobese diabetic (NOD)–severe combined immunodeficient (scid) IL-2 receptor-γ^{null} (NSG) mice. These mice have a severe grade of immunodeficiency, which allows for the engraftment of mature human immune cells. Once engrafted, the human cells can then mount alloimmunity against the transplanted human skin grafts. Seven days after the skin transplants, we intravenously injected T_{reg}-depleted peripheral blood mononuclear cells (PBMCs) and T_{regs} from the same donor, with or without IL-2/Fc NG conjugation, or we systemically supplemented the control T_{regs} with soluble IL-2/Fc (Fig. 5A). On day 21 after the adoptive T cell transfer, we analyzed the spleens and skin grafts of the NSG mice (Fig. 5B and fig. S11), being restricted to these draining sites due to the atrophy of secondary lymphoid tissues apart from the spleen in NSG mice.

By histology, the allografts of the CT- and CT + IL-2/Fc–treated conditions compared with healthy, untreated, untransplanted "naïve" human skin showed signs of epidermal-dermal interface changes, the abolishment of the rete ridges, adnexal disruption, spongiosis, dense lymphocytic infiltrates, and overall epidermal necrosis—all markers of severe rejection (Fig. 5C). The infiltration of T cells under these conditions was assessed by $CD3\varepsilon^+$ immunofluorescence staining, validating the presence of $CD3\varepsilon^+$ T cells in both CT- and CT + IL-2/Fc–treated mice (Fig. 5C). However, despite early signs of flattening of the rete ridges and mild spongiosis among the allografts of the NG-treated mice, there was no noticeable involvement of the overlying epidermis, no or rare lymphocytic infiltrates, limited adnexal involvement, and a well-demarcated reticular dermis, indicating healthier skin than under the CT-treated conditions with only mild grades of alloimmune-associated damage. In addition, using confocal microscopy, we observed $Foxp3^+$ cells in the allografts of NG-treated mice at the interface of the dermis and the graft bed (fig. S12A). There were also $Foxp3^+$ cells in the allografts of the CT + IL-2/Fc–treated mice; however, the incidence of allograft rejection was not attenuated in these mice, with 25% of the CT + IL-2/Fc grafts looking healthy versus 40% of the CT grafts and 80% of the NG grafts (Fig. 5D). Moreover, in bulk RNA extracted from the intact human skin allografts of CT T_{reg}– and NG T_{reg}–treated mice, we screened for the mRNA of several secreted and surface-bound proteins in the graft microenvironment, finding increased mRNA concentrations of *IL-1α*, *IL-7*, *TGF-β*, and *Foxp3*, as well as decreased E-selectin concentrations in the NG grafts compared with the CT grafts (fig. S12B).

By flow cytometry (fig. S11), we then analyzed the percentages of human $CD4^+Foxp3^+$ T_{regs} and $CD8\alpha^+$ T cells within the distal spleens and proximal skin allografts, as well as the ratio of T_{reg} to CD8α T cells in both draining sites, in which the T_{reg}-to-CD8α ratios were normalized against the CT-treated group to report the fold change differences. Similar to the in vivo murine T_{reg} results, we found that the systemic IL-2/Fc injection increased human T_{reg} percentages in the spleens of the NSG mice (Fig. 5E) and decreased $CD8\alpha^+$ percentages (Fig. 5F). This increase in T_{regs} and decrease in $CD8\alpha^+$ T cells improved the T_{reg}-to-CD8α ratios for the CT + IL-2/Fc mice in the spleens (Fig. 5, G to I). Preferential on-target, allograft-specific effects, as judged by increased T_{reg}-to-CD8α ratios in the allografts of the transplanted mice, however, were only observed under the NG-treated condition (Fig. 5, E to I). Last, complementing these histological and phenotypic findings was the observation that NG-treated mice had larger allografts at the time of the study end point (fig. S12C).

DISCUSSION

In recent years, cell-based T_{reg} therapy has moved to the frontiers of treatment strategies for auto- and alloimmune-mediated diseases (*6*). In contrast to drug-based approaches, adoptive T_{reg} transfer has the potential to induce permanent antigen-specific regulation of the immune system, which is a clinically unmet need in autoimmunity and transplantation. Nonetheless, the clinical success of this regulatory immunotherapy has been hampered by the poor in vivo homeostasis of the adoptively transferred T_{regs}, because T_{regs} rapidly disappear from the circulation upon adoptive transfer (*52*). Alternative immunotherapeutic strategies include the boosting of native T_{regs} within the immune system through systemic IL-2 injections, although this approach is accompanied by its own limitations. Excess concentrations of circulating IL-2 cause indirect endothelial cell damage through cytokines and vasoactive mediators originating from the nonspecific activation of NK cells and can also cause direct vascular damage secondary to the binding of IL-2 to $CD25^+$ endothelial cells (*50*). For over 20 years, this sequence of events has been termed vascular leak syndrome, and it remains one of the most serious side effects of IL-2 immunotherapy, known to precipitate organ failure due to the extravasation of fluids and proteins with subsequent interstitial edema (*53*). Here, we described an immunotherapeutic platform that can improve the potency of adoptive T_{reg} transfer and the on-target effects of systemic IL-2 therapy, by forming a combination therapy in which IL-2 release is linked explicitly to TCR ligation of adoptively transferred, antigen-specific T_{regs} in the allografts and graft-draining lymph nodes.

The goal of this technology is to improve the therapeutic outcomes of T_{reg} therapy without the need for genetic engineering, where cell surface–conjugated NGs (fig. S13A) provide a simple platform to enhance T_{reg} therapy. The critical factor in realizing this

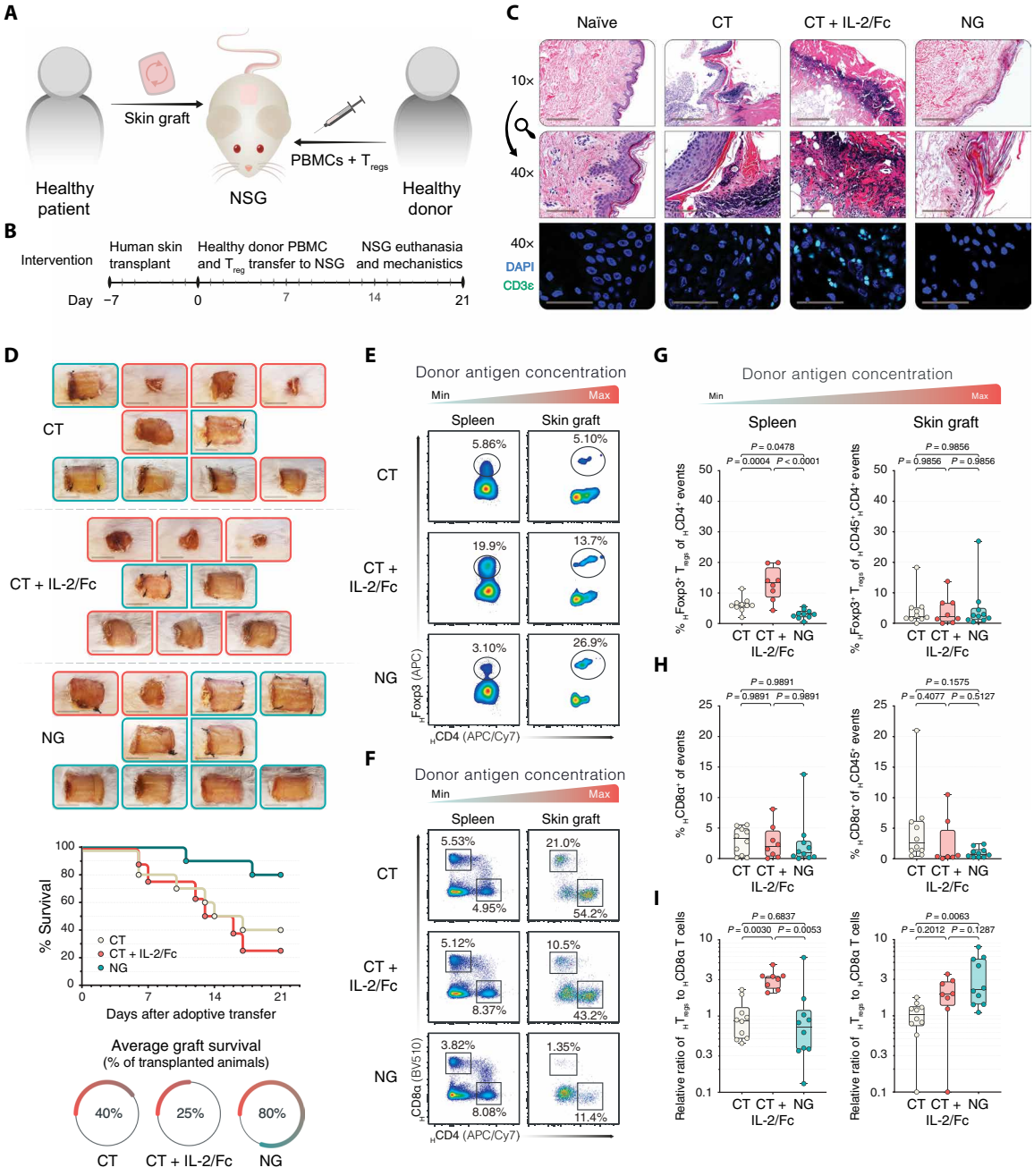

Fig. 5. Human T_{regs} coupled with IL-2/Fc NGs have improved function and homeostasis in vivo and promote intragraft T_{regs} in a humanized mouse model of skin transplantation. NSG mice were transplanted with skin grafts from healthy donors 7 days before the adoptive transfer of 5.0×10^6 $CD25^+CD127^{lo}$-depleted PBMCs and 1.0×10^6 T_{regs}, with or without IL-2/Fc NG, or with systemic IL-2/Fc. On day 21, the mice were euthanized, and various tissues were analyzed by histology, immunofluorescence, and flow cytometry ($n = 8$ to 10 biological replicates per condition, 2 experiments). (**A** and **B**) Experimental humanized mouse model (A) and time line (B). (**C**) H&E and CD3ε immunofluorescence staining of the experimental conditions and naïve, healthy human skin. Scale bars, 400 μm (10× H&E), 100 μm (40× H&E), and 40.0 μm (40× immunofluorescence). (**D**) Macroscopic images of each human skin allograft for all three treatment conditions at the experimental end point with red box borders indicating rejection, in addition to the survival curves and percentages on day 21. Scale bar, 10.0 mm. (**E** and **F**) Flow cytometric analyses of $Foxp3^+$ T_{regs} among $CD4^+$ lymphocytes (E) and $CD8\alpha^+$ T cells among all lymphocytes (F) in the spleens and skin grafts of the CT-, CT + IL-2/Fc–, and NG-treated NSG mice. (**G** to **I**) Box plots of $Foxp3^+$ percentages among $CD4^+$ events (G), $CD8\alpha^+$ T cells among all events (H), and fold changes of the T_{reg}-to-CD8α ratios in the distal and proximal draining sites (I). All fold changes were normalized against the CT condition. Throughout, data represented as boxplots with median, interquartile range, minimum, maximum, and all individual data points of the denoted experimental groups. *P* values were calculated with one-way analyses of variance followed by Holm-Šídák multiple comparison tests. NSG, NOD-scid IL-2 receptor-γ^{null}; PBMCs, peripheral blood mononuclear cells.

technology is the fact that T_{regs}, similar to other T lymphocytes, increase their cell surface reducing activity upon TCR ligation (fig. S13, B and C). The latter enables the exploitation of the naturally augmented redox potential on the surface of T_{regs} interacting with cognate antigens in the alloimmune environment and, thus, spatiotemporal control of IL-2 supplementation in a redox-sensitive, TCR-dependent fashion (fig. S13, D and E). Another essential characteristic of the NG platform is the short time required to modify the T_{regs} destined for adoptive transfer. A 45-min incubation was sufficient to conjugate >90% of T_{regs} with IL-2 NGs, with in vivo improvements in cell function and homeostasis and as much as three times increased survival outcomes in a murine skin allotransplantation model. The intuitive redox-sensitive backbone of the NGs provides a simple solution to a complex problem of enhancing T_{reg} functionality in proximal sites of inflammation, enabling on-target effects despite systemic injections.

In our in vivo murine experiments, we observed clear spatiotemporal benefits provided to the T_{regs} conjugated with IL-2 NGs, because there was an increase in the activation of NG T_{regs} in those tissues with the highest concentrations of alloantigen. In addition, across all in vivo experiments, an inverse relationship between the number of T_{regs} and CD8α T cells was only observed in the allografts and graft-draining lymph nodes of NG-treated mice. Furthermore, comparing the T_{reg}-to-CD8α ratios in the skin grafts of the transplant recipients to the T_{reg}-to-CD8α ratios in the spleens, we only found a >10-fold increase in the skin-to-spleen ratio in the mice treated with IL-2/Fc NG-engineered T_{regs}. This preferential on-target effect is intriguing, because mice treated with systemic IL-2/Fc had similarly increased numbers of T_{regs} but lower ratios of $Foxp3^+$ T_{regs} to CD8α T cells. Isolated increases in T_{reg} percentages in the $CD4^+$ compartment are not a reliable marker of downstream therapeutic effects. Clinically, increases in Foxp3 expression in the grafts and urine of kidney transplant recipients are used as biomarkers of allograft rejection (*54*, *55*). Through the restricted release of survival cytokines to alloantigen-specific T_{regs}, the NG platform proved capable of improving the ratio of $Foxp3^+$ T_{regs} to CD8α T cells—a more clinically relevant metric of therapeutic outcome (*56*).

From a translational perspective, we found that the murine results could be reproduced in human in vitro and humanized mouse in vivo settings. Besides confirming the preferential on-target effects of the IL-2/Fc NG-conjugated T_{regs}, there was an up-regulation of mRNA signatures in line with immune tolerance in NG-treated skin allografts. We observed increased transforming growth factor–β (TGF-β), known to inhibit antigen-presenting cell activity and confer "infectious tolerance" to neighboring cells (*57*, *58*), and Foxp3, a hallmark of the T_{reg} population (*1*–*3*). In addition, we found a decrease in the E-selectin expression, which facilitates the binding of immune cells to endothelial cells at sites of inflammation (*59*) and is positively correlated with the severity of allograft rejection (*60*). Last, we observed an increase in *IL-7* mRNA, which is a compelling finding in the context of recent studies that established IL-7 signaling as a key factor in maintaining the local T cell homeostasis of intragraft T_{regs} in mice (*61*, *62*). Although these findings remain to be validated in humans, it is becoming increasingly evident that the enhancement of adoptive T cell therapies requires a myriad of cytokine signals at different stages and in distinct locations. Because IL-7 is known for its role in stabilizing T cells of the memory phenotype, heightened IL-7 signaling could improve the maintenance of T_{regs} that have committed to peripheral tissues. The IL-2/Fc NGs were a test bed drug cargo to establish whether NGs could quickly and stably be tethered onto the T_{reg} surface without a loss of the host cell's phenotype or functionality.

Regarding the limitations, a fundamental constraint of the NG platform is, perhaps, its inherent self-limiting nature, because every division of the conjugated host cell dilutes the total surface-bound NGs (fig. S14A). Although we observed that IL-2/Fc NG-engineered T_{regs} ameliorated allograft acceptance outcomes in in vivo models compared with unmodified T_{regs} and T_{regs} supplemented with systemic IL-2/Fc, the effects of the IL-2/Fc NGs can last only as long as the supply of IL-2/Fc in the NG backpacks. Considering T_{reg} viability is innately linked to the continuity of IL-2 signaling, future efforts will be needed to optimize the release kinetics of the IL-2/Fc cargo from backpacked NGs. We postulate that altering the biochemical qualities of the cross-linkers that make up the IL-2/Fc NGs could further improve the homeostasis of NG T_{regs} and enable an equilibrium between the suppressive effects of the NG T_{regs} and their longevity. Alternatively, the self-limiting element of the NGs can be considered a natural safety mechanism in which the lifespan of the host cells and the number of cell divisions limit the effects of the membrane-tethered NGs. In addition, we can envision the option of multiple therapeutic injections of NG-coupled T_{regs} to realize longer-lasting effects of IL-2/Fc NG-conjugated T_{regs} while balancing the inherent temporal limitations of the NGs. Last, future experiments are essential to expand on the preliminary results we presented regarding the potential paracrine effects facilitated by IL-2/Fc NG-backpacked T_{regs}. Because the release of IL-2/Fc from the NG backpacks is mediated by reducing agents at the surface of the backpacked T_{regs}, robust activation of the IL-2/Fc NG-engineered T_{regs} could result in the off-target, paracrine IL-2–mediated stimulation of neighboring effector T cells by IL-2/Fc shedding from the NG backpacks (fig. S14B). On the other hand, activated effector T cells in the vicinity of naïve IL-2/Fc NG-engineered T_{regs} could nonspecifically consume the backpacked IL-2/Fc through an increased redox potential at their cell surface (fig. S14C).

Beyond the current limitations of the IL-2/Fc NG platform that require to be addressed in future studies, the overarching allure of this approach is its modularity and the potential to backpack alternative cytokines or biomolecules as adducted prodrugs for release in sites of antigen encounter (fig. S14D). For example, it can be envisioned that alternative cytokine-NG formulations such as IL-7 NGs can enhance the maintenance of tissue-specific T_{regs} or, perhaps, that formulations with IL-10 or TGF-β can promote the induction of paracrine infectious tolerance within the alloimmune microenvironment and, lastly, that formulations with adjuvants or immunosuppressive drugs can allow backpacked T_{regs} to act as mules in delivering immunostimulatory or immunosuppressive payloads in situ.

In all, the NG platform holds potential therapeutic merit in tackling diseases of an auto- or alloimmune nature, providing its effects in controlled spaces by linking innate TCR signaling to the release of immunomodulatory proteins. In addition, it is critical to note that most of the results in this work demonstrate the efficacy of the platform in improving the outcomes of polyclonal T_{reg} transfer. Using an artificial antigen-specific allotransplant model in this study, we already observed the heightened effects of engineering IL-2/Fc NGs on antigen-specific T_{regs}. Hence, we can foresee our platform being complementary to chimeric antigen-specific T_{regs} (*63*, *64*) to create a combination therapy that has the potential to induce tolerogenic

responses and achieve even longer-lasting allograft acceptance (fig. S14E).

MATERIALS AND METHODS

Study design

This study was designed to investigate T_{regs} engineered with surface-conjugated, nanoscale IL-2 particles compared with unmodified T_{regs} as immunoregulatory adoptive cell therapy in the context of allotransplantation. To this end, NG IL-2/Fc fusion NG particles were synthesized with reduction-sensitive bis-NHS cross-linkers that degrade upon TCR ligation–dependent T cell activation. Then, the ability to couple NG particles on T_{regs} was verified, and unaltered functional characteristics of coupled T_{regs} were confirmed with in vitro survival and suppression assays. NG T_{reg} functionality in vivo was tested in *Rag1*$^{-/-}$ mice transplanted with fully MHC-mismatched skin and humanized NSG mice transplanted with the human skin. Specifically, we focused on the efficacy of NG-coupled T_{regs} to suppress local proinflammatory T cells in sites of antigen encounter, including the allograft, without activating peripheral T_{regs}. To assess the survival benefits to the allograft, we performed survival studies with an allogeneic skin transplant model. Animals were assigned to treatment groups randomly and age-matched between conditions where necessary. The investigators were not blinded, sample sizes were not predetermined by power analysis in light of prior experience, and no animals were excluded because of illness.

Mice

C57BL/6 (#000664), *BALB/c* (#000651), *B6.129S7-Rag1*^{tm1Mom} (*Rag1*$^{-/-}$; #002216), *C57BL/6-Tg(CAG-OVA)916Jen* (OVA; #005145), *C57BL/6-Tg(TcraTcrb)1100Mjb* (OT-1; #003831), *B6.Cg-Tg(TcraTcrb)425Cbn* (OT-2; #004194), and *NOD.Cg-Prkdc*^{scid} *Il2rg*^{tm1Wjl}*/Sz* (NSG; #005557) mice were purchased from the Jackson laboratories. All murine strains in this study were maintained under specific pathogen–free conditions at the Brigham and Women's Hospital animal facility in accordance with federal, state, and institutional guidelines. The study protocol was approved by the Brigham and Women's Hospital Institutional Animal Care and Use Committee. Mice were sex- and age-matched (8 to 12 weeks old) apart from several NSG mice that were up to 6 months of age (these mice were equally randomized into the treatment groups for the humanized experiments).

Human individuals and blood samples

Concentrated, leukapheresed blood from healthy individuals was obtained from the Brigham and Women's Hospital Blood Bank for the in vitro human and in vivo humanized experiments. PBMCs were isolated from the leukapheresed concentrates within 4 hours by SepMate tubes (STEMCELL Technologies, #85450). Healthy skin was obtained from patients undergoing cosmetic surgery procedures as discarded tissues at the Brigham and Women's Hospital Plastic Surgery Division. The study protocol was approved by an Institutional Review Board at the Brigham and Women's Hospital and was performed in accordance with the principles of the Declaration of Helsinki.

Synthesis of NGs

Bis-NHS cross-linkers (details provided in Supplementary Materials and Methods) were dissolved at 10 mg/ml in dimethyl sulfoxide and added to an IL-2/Fc solution [10 mg/ml in 1× Dulbecco's phosphate buffered saline (DPBS)] at a molar equivalent of 15:1 cross-linker–to–IL-2/Fc ratio. The cocktail was rotated at 25°C for 30 min, at which point 1× DPBS was added to bring the final protein concentration to 1 mg/ml. Subsequently, anti-CD45 in 1× DPBS was added to the diluted solution at a 1:10 molar equivalent of anti-CD45–to–IL-2/Fc ratio, and the reaction mixture was rotated at 25°C for another 30 min. The resulting NGs were then washed thrice with 1.5 ml of 1× DPBS in a 100-kDa molecular weight cutoff Amicon ultracentrifugal filter (Millipore, #UFC910024). To enhance conjugation of anti-CD45/IL-2/Fc-NGs to T cells, before T cell coupling, polyethylene glycol–*b*-polylysine (PEG5k-PLL33k) in 1× DPBS was mixed with freshly prepared NGs at a 12.5:100 molar equivalent of PEG-PLL–to–IL-2/Fc ratio. The mixture was rotated at 25°C for 2 to 16 hours and used without further purification.

Coupling of NGs

Engineering of the T_{reg} surface with IL-2/Fc NGs was performed immediately before intravenous adoptive transfer. Briefly, freshly magnetically sorted T_{regs} were divided into two groups, control (CT) and NG. NG T_{regs} were routinely coupled with 10 to 20 μg of NG/10^6 T_{regs} in 200 μl of 1× Hanks' balanced salt solution (HBSS) (Gibco, #14175095). CT T_{regs} were similarly suspended in 200 μl of 1× HBSS, however, in the absence of NGs. Both T_{reg} groups were then incubated at 4°C on an intermediate speed plate shaker (setting 7/10) for 45 min. Consistently, nearly half of all CT and NG T_{regs} were lost during the coupling step. After coupling, CT and NG T_{regs} were washed twice with 1× DPBS and used for downstream in vitro and in vivo applications.

Skin transplant models

To study the efficacy of the NG platform in controlling alloimmune responses, we used a fully MHC-mismatched murine skin transplant model. Full-thickness trunk skin grafts (1.0 cm by 1.5 cm) from BALB/c donors were harvested at the level of the areolar connective tissue, and connective, adipose, and panniculus carnosus tissues were cleared using blunt-tipped forceps. The fur of each anesthetized recipient *Rag1*$^{-/-}$ mouse was shaven at the dorsal trunk, 1.0 cm by 1.5 cm of the recipient mouse's skin was excised, and an equally sized skin graft was sutured onto the graft bed with PERMA-HAND 4-0 Silk Suture (Ethicon, #1677G). Skin transplants were secured with dry gauze and bandaged for 7 to 10 days. For survival studies, grafts were monitored daily for the presence of erythema, erosion, contraction, or necrosis of the allografts. In addition, antigen-specific alloimmune responses were studied with OVA donor grafts and *Rag1*$^{-/-}$ recipients, whereas human alloimmune responses were assessed with human skin grafts (obtained as described above) and NSG recipients, as described above.

Adoptive T_{reg} transfer models

For the polyclonal T_{reg} experiments, 5.0×10^5 CD8α$^+$ cells and 5.0×10^5 CD4$^+$CD25$^+$ T_{regs} with or without IL-2/Fc NG from C57BL/6 mice were injected retro-orbitally in 90-μl total volumes of 1× DPBS at day 3 after transplant. For methodological reasons, larger cell numbers could not be obtained. As a control condition, a group of CT T_{reg}–treated mice received intravenous free IL-2/Fc at the time of the adoptive transfer, in the same total concentration as would be released from the IL-2/Fc NG coupled to the NG T_{regs}. With an average IL-2/Fc release of 90% from the NG particles after 7 days and 90% of the NG T_{regs} being conjugated with IL-2/Fc NGs,

together with 10 μg of NGs being conjugated with 10^6 T_{regs}, for every mouse injected with 5.0×10^5 NG T_{regs}, 5.0×10^5 CT T_{regs} were coinjected with 4.1 μg of free IL-2/Fc and referred to in the manuscript as CT + IL-2/Fc T_{regs}. This was considered the equivalent dose of IL-2/Fc under the CT + IL-2/Fc and NG conditions.

Animals were euthanized at day 7 after adoptive transfer for mechanistic studies and left until allograft rejection in survival studies. For the antigen-specific T_{reg} experiments, 5.0×10^5 $CD8\alpha^+$ cells and 2.5×10^5 $CD4^+CD25^+$ T_{regs} with or without IL-2/Fc NG from OT-1 mice and 2.5×10^5 $CD4^+CD25^+$ T_{regs} with or without IL-2/Fc NG from OT-2 mice were injected retro-orbitally in 90-μl total volumes of 1× DPBS 3 days after transplant. Animals were euthanized at day 7 after adoptive transfer for mechanistic studies.

For the humanized T_{reg} experiments, 5.0×10^6 $CD25^+CD127^{lo}$-depleted PBMCs and 1.0×10^6 $CD25^+CD127^{lo}$ T_{regs} from a healthy donor were injected retro-orbitally in 90-μl total volumes of 1× DPBS 7 days after transplant. Animals were euthanized at day 21 after adoptive transfer for mechanistic studies.

Statistics

Differences between two normally distributed groups were analyzed with independent samples two-tailed Student's *t* tests, and nonparametric Kolmogorov-Smirnov tests were performed when the assumption of homoscedasticity could not be met. Statistical analyses of multiple groups were performed with one-way analyses of variance followed by Holm-Šídák multiple comparison tests or mixed-effects model analyses with the Geisser-Greenhouse correction followed by Holm-Šídák multiple comparison tests for experimental groups with matched data points across multiple time points or concentrations. Fold changes were normalized against the CT condition unless otherwise specified. To study the correlation between the suppressive profiles of CT and NG T_{regs}, CT and NG proliferation indices at the same suppressor-to-responder ratios were plotted against each other, and through linear regression, Pearson's correlation coefficient (R) was calculated. For survival analyses, Kaplan-Meier graphs were analyzed with log-rank Mantel-Cox tests. $P < 0.05$ was considered significant for all analyses. Data analysis and graphing were performed with Prism 8.0 (GraphPad Software). Graphs show boxplots with median, interquartile range, minimum, maximum, and all individual data points of the denoted experimental groups. Original data are provided in data file S1.

Additional experimental details are provided in Supplementary Materials and Methods.

SUPPLEMENTARY MATERIALS

stm.sciencemag.org/cgi/content/full/12/569/eaaw4744/DC1
Materials and Methods
Fig. S1. Murine in vitro T_{reg} and T cell phenotyping strategy.
Fig. S2. IL-2/Fc release from NGs and NG surface retention on engineered T_{regs}.
Fig. S3. IL-2/Fc NGs promote the maintenance of T_{reg} survival and phenotype in a CD3ε dose-dependent fashion.
Fig. S4. Splenic T cell suppression correlation analysis.
Fig. S5. Murine in vivo skin transplant model phenotyping strategy.
Fig. S6. NG-conjugated T_{regs} proliferate optimally in proximal sites of alloimmunity with decreased CD8α T cells and unaffected NK cells.
Fig. S7. Synchronously tracking T_{regs} and CD8 T cells with bioluminescent luciferase reporters.
Fig. S8. Antigen-specific mouse model of skin transplantation phenotyping strategy.
Fig. S9. Antigen-specific nanogeled T cells proliferate better in proximal sites of alloimmunity than nonantigen-specific nanogeled T cells.
Fig. S10. IL-2/Fc NGs conjugated to human T_{regs} improve their in vitro homeostasis compared to conventional T_{regs}.
Fig. S11. In vivo humanized mouse model of human skin transplantation phenotyping strategy.
Fig. S12. In vivo IL-2/Fc NG treatment of humanized skin transplanted mice favors graft size maintenance and intragraft T_{reg} dominance over conventional T_{reg} treatments.
Fig. S13. NG backpacks are quickly and stably tethered on T_{regs} to facilitate the spatiotemporal release of adducted prodrugs at sites of antigen encounter.
Fig. S14. Limitations and future perspectives for IL-2/Fc NG–based immunotherapy.
Table S1. Full list of the microscopy antibodies used in this study.
Table S2. Full list of the flow cytometry antibodies used in this study.
Table S3. Full list of the mRNA transcript targets and primers used in this study.
Table S4. Two-step quantitative real-time polymerase chain reaction protocol.
Data file S1. Original data.
Movie S1. Three-dimensional volume view of control T_{reg} after in vitro coupling.
Movie S2. Three-dimensional volume view of NG-conjugated T_{reg} after in vitro coupling.
References (*65*–*68*)

View/request a protocol for this paper from *Bio-protocol*.

REFERENCES AND NOTES

1. S. Sakaguchi, N. Sakaguchi, M. Asano, M. Itoh, M. Toda, Immunologic self-tolerance maintained by activated T cells expressing IL-2 receptor alpha-chains (CD25). Breakdown of a single mechanism of self-tolerance causes various autoimmune diseases. *J. Immunol.* **155**, 1151–1164 (1995).
2. S. Hori, T. Nomura, S. Sakaguchi, Control of regulatory T cell development by the transcription factor *Foxp3*. *Science* **299**, 1057–1061 (2003).
3. J. D. Fontenot, M. A. Gavin, A. Y. Rudensky, Foxp3 programs the development and function of $CD4^+CD25^+$ regulatory T cells. *Nat. Immunol.* **4**, 330–336 (2003).
4. K. J. Wood, S. Sakaguchi, Regulatory T cells in transplantation tolerance. *Nat. Rev. Immunol.* **3**, 199–210 (2003).
5. S. Sakaguchi, T. Yamaguchi, T. Nomura, M. Ono, Regulatory T cells and immune tolerance. *Cell* **133**, 775–787 (2008).
6. K. J. Wood, A. Bushell, J. Hester, Regulatory immune cells in transplantation. *Nat. Rev. Immunol.* **12**, 417–430 (2012).
7. P. Trzonkowski, M. Bieniaszewska, J. Juścińska, A. Dobyszuk, A. Krzystyniak, N. Marek, J. Myśliwska, A. Hellmann, First-in-man clinical results of the treatment of patients with graft versus host disease with human ex vivo expanded $CD4^+CD25^+CD127^-$ T regulatory cells. *Clin. Immunol.* **133**, 22–26 (2009).
8. N. Marek-Trzonkowska, M. Myśliwiec, A. Dobyszuk, M. Grabowska, I. Derkowska, J. Juścińska, R. Owczuk, A. Szadkowska, P. Witkowski, W. Młynarski, P. Jarosz-Chobot, A. Bossowski, J. Siebert, P. Trzonkowski, Therapy of type 1 diabetes with $CD4^+CD25^{high}CD127$-regulatory T cells prolongs survival of pancreatic islets - results of one year follow-up. *Clin. Immunol.* **153**, 23–30 (2014).
9. L. Graca, S. P. Cobbold, H. Waldmann, Identification of regulatory T cells in tolerated allografts. *J. Exp. Med.* **195**, 1641–1646 (2002).
10. M. Carvalho-Gaspar, N. D. Jones, S. Luo, L. Martin, M. O. Brook, K. J. Wood, Location and time-dependent control of rejection by regulatory T cells culminates in a failure to generate memory T cells. *J. Immunol.* **180**, 6640–6648 (2008).
11. M. D. Rosenblum, I. K. Gratz, J. S. Paw, K. Lee, A. Marshak-Rothstein, A. K. Abbas, Response to self antigen imprints regulatory memory in tissues. *Nature* **480**, 538–542 (2011).
12. J. L. Riley, C. H. June, B. R. Blazar, Human T regulatory cell therapy: Take a billion or so and call me in the morning. *Immunity* **30**, 656–665 (2009).
13. C. McDonald-Hyman, L. A. Turka, B. R. Blazar, Advances and challenges in immunotherapy for solid organ and hematopoietic stem cell transplantation. *Sci. Transl. Med.* **7**, 280rv2 (2015).
14. N. Safinia, N. Grageda, C. Scottà, S. Thirkell, L. J. Fry, T. Vaikunthanathan, R. I. Lechler, G. Lombardi, Cell therapy in organ transplantation: Our experience on the clinical translation of regulatory T cells. *Front. Immunol.* **9**, 354 (2018).
15. Q. Tang, K. Lee, Regulatory T-cell therapy for transplantation: How many cells do we need? *Curr. Opin. Organ Transplant.* **17**, 349–354 (2012).
16. Q. Tang, J. A. Bluestone, Regulatory T-cell therapy in transplantation: Moving to the clinic. *Cold Spring Harb. Perspect. Med.* **3**, a015552 (2013).
17. O. Joffre, T. Santolaria, D. Calise, T. Al Saati, D. Hudrisier, P. Romagnoli, J. P. M. van Meerwijk, Prevention of acute and chronic allograft rejection with $CD4^+CD25^+Foxp3^+$ regulatory T lymphocytes. *Nat. Med.* **14**, 88–92 (2008).
18. H. Allos, B. S. Al Dulaijan, J. Choi, J. Azzi, Regulatory T cells for more targeted immunosuppressive therapies. *Clin. Lab. Med.* **39**, 1–13 (2019).
19. N. Komatsu, M. E. Mariotti-Ferrandiz, Y. Wang, B. Malissen, H. Waldmann, S. Hori, Heterogeneity of natural $Foxp3^+$ T cells: A committed regulatory T-cell lineage and an uncommitted minor population retaining plasticity. *Proc. Natl. Acad. Sci. U.S.A.* **106**, 1903–1908 (2009).
20. X. Zhou, S. L. Bailey-Bucktrout, L. T. Jeker, C. Penaranda, M. Martínez-Llordella, M. Ashby, M. Nakayama, W. Rosenthal, J. A. Bluestone, Instability of the transcription factor Foxp3

leads to the generation of pathogenic memory T cells *in vivo*. *Nat. Immunol.* **10**, 1000–1007 (2009).
21. E. Bettelli, Y. Carrier, W. Gao, T. Korn, T. B. Strom, M. Oukka, H. L. Weiner, V. K. Kuchroo, Reciprocal developmental pathways for the generation of pathogenic effector T_H17 and regulatory T cells. *Nature* **441**, 235–238 (2006).
22. S. Z. Josefowicz, L.-F. Lu, A. Y. Rudensky, Regulatory T cells: Mechanisms of differentiation and function. *Annu. Rev. Immunol.* **30**, 531–564 (2012).
23. J. C. Vahl, C. Drees, K. Heger, S. Heink, J. C. Fischer, J. Nedjic, N. Ohkura, H. Morikawa, H. Poeck, S. Schallenberg, D. Rieß, M. Y. Hein, T. Buch, B. Polic, A. Schönle, R. Zeiser, A. Schmitt-Gräff, K. Kretschmer, L. Klein, T. Korn, S. Sakaguchi, M. Schmidt-Supprian, Continuous T cell receptor signals maintain a functional regulatory T cell pool. *Immunity* **41**, 722–736 (2014).
24. A. G. Levine, A. Arvey, W. Jin, A. Y. Rudensky, Continuous requirement for the TCR in regulatory T cell function. *Nat. Immunol.* **15**, 1070–1078 (2014).
25. R. Setoguchi, S. Hori, T. Takahashi, S. Sakaguchi, Homeostatic maintenance of natural *Foxp3*$^+$ CD25$^+$ CD4$^+$ regulatory T cells by interleukin (IL)-2 and induction of autoimmune disease by IL-2 neutralization. *J. Exp. Med.* **201**, 723–735 (2005).
26. O. Boyman, M. Kovar, M. P. Rubinstein, C. D. Surh, J. Sprent, Selective stimulation of T cell subsets with antibody-cytokine immune complexes. *Science* **311**, 1924–1927 (2006).
27. M. A. Burchill, J. Yang, C. Vogtenhuber, B. R. Blazar, M. A. Farrar, IL-2 receptor β-dependent STAT5 activation is required for the development of Foxp3$^+$ regulatory T cells. *J. Immunol.* **178**, 280–290 (2007).
28. A. M. Thornton, E. M. Shevach, CD4$^+$CD25$^+$ immunoregulatory T cells suppress polyclonal T cell activation in vitro by inhibiting interleukin 2 production. *J. Exp. Med.* **188**, 287–296 (1998).
29. Y. P. Rubtsov, R. E. Niec, S. Josefowicz, L. Li, J. Darce, D. Mathis, C. Benoist, A. Y. Rudensky, Stability of the regulatory T cell lineage in vivo. *Science* **329**, 1667–1671 (2010).
30. K.-i. Matsuoka, J. Koreth, H. T. Kim, G. Bascug, S. M. Donough, Y. Kawano, K. Murase, C. Cutler, V. T. Ho, E. P. Alyea, P. Armand, B. R. Blazar, J. H. Antin, R. J. Soiffer, J. Ritz, Low-dose interleukin-2 therapy restores regulatory T cell homeostasis in patients with chronic graft-versus-host disease. *Sci. Transl. Med.* **5**, 179ra43 (2013).
31. D. Klatzmann, A. K. Abbas, The promise of low-dose interleukin-2 therapy for autoimmune and inflammatory diseases. *Nat. Rev. Immunol.* **15**, 283–294 (2015).
32. J. Koreth, H. T. Kim, K. T. Jones, P. B. Lange, C. G. Reynolds, M. J. Chammas, K. Dusenbury, J. Whangbo, S. Nikiforow, E. P. Alyea III, P. Armand, C. S. Cutler, V. T. Ho, Y.-B. Chen, D. Avigan, B. R. Blazar, J. H. Antin, J. Ritz, R. J. Soiffer, Efficacy, durability, and response predictors of low-dose interleukin-2 therapy for chronic graft-versus-host disease. *Blood* **128**, 130–137 (2016).
33. G. Camirand, L. V. Riella, Treg-centric view of immunosuppressive drugs in transplantation: A balancing act. *Am. J. Transplant.* **17**, 601–610 (2017).
34. M. Hirakawa, T. R. Matos, H. Liu, J. Koreth, H. T. Kim, N. E. Paul, K. Murase, J. Whangbo, A. C. Alho, S. Nikiforow, C. Cutler, V. T. Ho, P. Armand, E. P. Alyea, J. H. Antin, B. R. Blazar, J. F. Lacerda, R. J. Soiffer, J. Ritz, Low-dose IL-2 selectively activates subsets of CD4$^+$ Tregs and NK cells. *JCI Insight* **1**, e89278 (2016).
35. L. Tang, Y. Zheng, M. B. Melo, L. Mabardi, A. P. Castaño, Y.-Q. Xie, N. Li, S. B. Kudchodkar, H. C. Wong, E. K. Jeng, M. V. Maus, D. J. Irvine, Enhancing T cell therapy through TCR-signaling-responsive nanoparticle drug delivery. *Nat. Biotechnol.* **36**, 707–716 (2018).
36. R. J. Noelle, D. A. Lawrence, Modulation of T-cell function: II. Chemical basis for the involvement of cell surface thiol-reactive sites in control of T-cell proliferation. *Cell. Immunol.* **60**, 453–469 (1981).
37. D. A. Lawrence, R. Song, P. Weber, Surface thiols of human lymphocytes and their changes after in vitro and in vivo activation. *J. Leukoc. Biol.* **60**, 611–618 (1996).
38. D. Mougiakakos, C. C. Johansson, R. Kiessling, Naturally occurring regulatory T cells show reduced sensitivity toward oxidative stress-induced cell death. *Blood* **113**, 3542–3545 (2009).
39. D. Mougiakakos, C. C. Johansson, R. Jitschin, M. Böttcher, R. Kiessling, Increased thioredoxin-1 production in human naturally occurring regulatory T cells confers enhanced tolerance to oxidative stress. *Blood* **117**, 857–861 (2011).
40. J. Xu, J. Wang, J. C. Luft, S. Tian, G. Owens Jr., A. A. Pandya, P. Berglund, P. Pohlhaus, B. W. Maynor, J. Smith, B. Hubby, M. E. Napier, J. M. DeSimone, Rendering protein-based particles transiently insoluble for therapeutic applications. *J. Am. Chem. Soc.* **134**, 8774–8777 (2012).
41. C. F. Riber, A. A. A. Smith, A. N. Zelikin, Self-immolative linkers literally bridge disulfide chemistry and the realm of thiol-free drugs. *Adv. Healthc. Mater.* **4**, 1887–1890 (2015).
42. L. Baudino, Y. Shinohara, F. Nimmerjahn, J.-I. Furukawa, M. Nakata, E. Martinez-Soria, F. Petry, J. V. Ravetch, S.-I. Nishimura, S. Izui, Crucial role of aspartic acid at position 265 in the CH2 domain for murine IgG2a and IgG2b Fc-associated effector functions. *J. Immunol.* **181**, 6664–6669 (2008).
43. J. W. Fabre, A. F. Williams, Quantitative serological analysis of a rabbit anti-rat lymphocyte serum and preliminary biochemical characterisation of the major antigen recognised. *Transplantation* **23**, 349–359 (1977).
44. M. L. Thomas, A. N. Barclay, J. Gagnon, A. F. Williams, Evidence from cDNA clones that the rat leukocyte-common antigen (T200) spans the lipid bilayer and contains a cytoplasmic domain of 80,000 M_r. *Cell* **41**, 83–93 (1985).
45. L. M. Francisco, V. H. Salinas, K. E. Brown, V. K. Vanguri, G. J. Freeman, V. K. Kuchroo, A. H. Sharpe, PD-L1 regulates the development, maintenance, and function of induced regulatory T cells. *J. Exp. Med.* **206**, 3015–3029 (2009).
46. T. Asano, Y. Meguri, T. Yoshioka, Y. Kishi, M. Iwamoto, M. Nakamura, Y. Sando, H. Yagita, J. Koreth, H. T. Kim, E. P. Alyea, P. Armand, C. S. Cutler, V. T. Ho, J. H. Antin, R. J. Soiffer, Y. Maeda, M. Tanimoto, J. Ritz, K.-I. Matsuoka, PD-1 modulates regulatory T-cell homeostasis during low-dose interleukin-2 therapy. *Blood* **129**, 2186–2197 (2017).
47. U. Grohmann, C. Orabona, F. Fallarino, C. Vacca, F. Calcinaro, A. Falorni, P. Candeloro, M. L. Belladonna, R. Bianchi, M. C. Fioretti, P. Puccetti, CTLA-4-Ig regulates tryptophan catabolism *in vivo*. *Nat. Immunol.* **3**, 1097–1101 (2002).
48. K. Wing, Y. Onishi, P. Prieto-Martin, T. Yamaguchi, M. Miyara, Z. Fehervari, T. Nomura, S. Sakaguchi, CTLA-4 control over Foxp3$^+$ regulatory T cell function. *Science* **322**, 271–275 (2008).
49. D. Cibrián, F. Sánchez-Madrid, CD69: From activation marker to metabolic gatekeeper. *Eur. J. Immunol.* **47**, 946–953 (2017).
50. N. Arenas-Ramirez, J. Woytschak, O. Boyman, Interleukin-2: Biology, design and application. *Trends Immunol.* **36**, 763–777 (2015).
51. H. Fujii, Y. Nakagawa, U. Schindler, A. Kawahara, H. Mori, F. Gouilleux, B. Groner, J. N. Ihle, Y. Minami, T. Miyazaki, Activation of Stat5 by interleukin 2 requires a carboxyl-terminal region of the interleukin 2 receptor beta chain but is not essential for the proliferative signal transmission. *Proc. Natl. Acad. Sci. U.S.A.* **92**, 5482–5486 (1995).
52. J. A. Bluestone, J. H. Buckner, M. Fitch, S. E. Gitelman, S. Gupta, M. K. Hellerstein, K. C. Herold, A. Lares, M. R. Lee, K. Li, W. Liu, S. A. Long, L. M. Masiello, V. Nguyen, A. L. Putnam, M. Rieck, P. H. Sayre, Q. Tang, Type 1 diabetes immunotherapy using polyclonal regulatory T cells. *Sci. Transl. Med.* **7**, 315ra189 (2015).
53. R. Baluna, E. S. Vitetta, Vascular leak syndrome: A side effect of immunotherapy. *Immunopharmacology* **37**, 117–132 (1997).
54. H. Mansour, S. Homs, D. Desvaux, C. Badoual, K. Dahan, M. Matignon, V. Audard, P. Lang, P. Grimbert, Intragraft levels of Foxp3 mRNA predict progression in renal transplants with borderline change. *J. Am. Soc. Nephrol.* **19**, 2277–2281 (2008).
55. T. Muthukumar, D. Dadhania, R. Ding, C. Snopkowski, R. Naqvi, J. B. Lee, C. Hartono, B. Li, V. K. Sharma, S. V. Seshan, S. Kapur, W. W. Hancock, J. E. Schwartz, M. Suthanthiran, Messenger RNA for FOXP3 in the urine of renal-allograft recipients. *N. Engl. J. Med.* **353**, 2342–2351 (2005).
56. C. C. Preston, M. J. Maurer, A. L. Oberg, D. W. Visscher, K. R. Kalli, L. C. Hartmann, E. L. Goode, K. L. Knutson, The ratios of CD8$^+$ T cells to CD4$^+$CD25$^+$ FOXP3$^+$ and FOXP3$^-$ T cells correlate with poor clinical outcome in human serous ovarian cancer. *PLOS ONE* **8**, e80063 (2013).
57. C. I. Kingsley, M. Karim, A. R. Bushell, K. J. Wood, CD25$^+$CD4$^+$ regulatory T cells prevent graft rejection: CTLA-4- and IL-10-dependent immunoregulation of alloresponses. *J. Immunol.* **168**, 1080–1086 (2002).
58. J. Andersson, D. Q. Tran, M. Pesu, T. S. Davidson, H. Ramsey, J. J. O'Shea, E. M. Shevach, CD4$^+$ FoxP3$^+$ regulatory T cells confer infectious tolerance in a TGF-β-dependent manner. *J. Exp. Med.* **205**, 1975–1981 (2008).
59. F. Austrup, D. Vestweber, E. Borges, M. Löhning, R. Bräuer, U. Herz, H. Renz, R. Hallmann, A. Scheffold, A. Radbruch, A. Hamann, P- and E-selectin mediate recruitment of T-helper-1 but not T-helper-2 cells into inflammed tissues. *Nature* **385**, 81–83 (1997).
60. T. Hautz, B. Zelger, J. Grahammer, C. Krapf, A. Amberger, G. Brandacher, L. Landin, H. Müller, M. P. Schön, P. Cavadas, A. W. P. Lee, J. Pratschke, R. Margreiter, S. Schneeberger, Molecular markers and targeted therapy of skin rejection in composite tissue allotransplantation. *Am. J. Transplant.* **10**, 1200–1209 (2010).
61. F. Carrette, C. D. Surh, IL-7 signaling and CD127 receptor regulation in the control of T cell homeostasis. *Semin. Immunol.* **24**, 209–217 (2012).
62. I. K. Gratz, H. A. Truong, S. H. Yang, M. M. Maurano, K. Lee, A. K. Abbas, M. D. Rosenblum, Cutting edge: Memory regulatory T cells require IL-7 and not IL-2 for their maintenance in peripheral tissues. *J. Immunol.* **190**, 4483–4487 (2013).
63. D. A. Boardman, C. Philippeos, G. O. Fruhwirth, M. A. Ibrahim, R. F. Hannen, D. Cooper, F. M. Marelli-Berg, F. M. Watt, R. I. Lechler, J. Maher, L. A. Smyth, G. Lombardi, Expression of a chimeric antigen receptor specific for donor HLA class i enhances the potency of human regulatory T cells in preventing human skin transplant rejection. *Am. J. Transplant.* **17**, 931–943 (2017).
64. F. Noyan, K. Zimmermann, M. Hardtke-Wolenski, A. Knoefel, E. Schulde, R. Geffers, M. Hust, J. Huehn, M. Galla, M. Morgan, A. Jokuszies, M. P. Manns, E. Jaeckel, Prevention of allograft rejection by use of regulatory T cells with an MHC-specific chimeric antigen receptor. *Am. J. Transplant.* **17**, 917–930 (2017).
65. Y. Zheng, M. T. Stephan, S. A. Gai, W. Abraham, A. Shearer, D. J. Irvine, *In vivo* targeting of adoptively transferred T-cells with antibody- and cytokine-conjugated liposomes. *J. Control. Release* **172**, 426–435 (2013).

66. J. Schindelin, I. Arganda-Carreras, E. Frise, V. Kaynig, M. Longair, T. Pietzsch, S. Preibisch, C. Rueden, S. Saalfeld, B. Schmid, J.-Y. Tinevez, D. J. White, V. Hartenstein, K. Eliceiri, P. Tomancak, A. Cardona, Fiji: An open-source platform for biological-image analysis. *Nat. Methods* **9**, 676–682 (2012).
67. F. de Chaumont, S. Dallongeville, N. Chenouard, N. Hervé, S. Pop, T. Provoost, V. Meas-Yedid, P. Pankajakshan, T. Lecomte, Y. L. Montagner, T. Lagache, A. Dufour, J.-C. Olivo-Marin, Icy: An open bioimage informatics platform for extended reproducible research. *Nat. Methods* **9**, 690–696 (2012).
68. T. Metsalu, J. Vilo, ClustVis: A web tool for visualizing clustering of multivariate data using principal component analysis and heatmap. *Nucleic Acids Res.* **43**, W566–W570 (2015).

Acknowledgments: We thank the Talal and Maha Shair Foundation for their support to science; our colleagues at the Schuster Family Transplantation Research Center at the Brigham and Women's Hospital for assistance and collaboration; the anonymous reviewers for constructive feedback; the patients who made this work possible in trusting us with their donated skin and blood samples; the Harvard Department of Immunology's Flow Cytometry Facility for assistance with the flow cytometric analyses; and S. Tripathi, N. Murakami, F. Ordikhani, A. Akbarzadeh, F. Juillard, and B. Liu for technical assistance in this study. D.J.I. is an investigator of the Howard Hughes Medical Institute. **Funding:** J.Y.C. was supported by the NIH (T32 DK007527). American Heart Association (AHA Award 13FTF17000018 to J.R.A.), American Diabetes Association (ADA Award 1-17-IBS-206 to J.R.A.), Qatar Foundation Grant (NPRP8-1744-3-357X to J.R.A.), and the NIH (RO1 AI134842 to J.R.A.). **Author contributions:** D.J.I. and J.R.A. formulated the overarching research aims. J.R.A. and S.K.E. designed the experimental models and analyzed and interpreted the data. H.A., I.S., J.B.A., M.B.M., N.L., and S.K.E. performed experiments and collected data. I.S. bred animals for the transgenic animal models. M.B.M. and N.L. synthesized NGs. A.M., A.S.E., B.K., B.P., B.S.A.D., J.P.A., J.Y.C., M.A.Z., M.B.M., S.C., and T.J.B. provided study materials, reagents, patient samples, instrumentation, or other analysis tools. J.R.A. and S.K.E. wrote the initial draft of the manuscript. B.A.T., B.P., H.G.D.L., L.T., L.V.R., M.A.J.S., W.J.v.S., and Y.H. critically reviewed the manuscript and provided commentary. D.J.I., I.S., J.R.A., M.B.M., and S.K.E. revised the manuscript and prepared it for publication. D.J.I., J.R.A., and M.A.J.S. supervised the study. J.R.A. acquired funding for the work presented in the manuscript. **Competing interests:** D.J.I. and L.T. are inventors on U.S. patent no. 2017/0080104 A1 ("Cell Surface Coupling of Nanoparticles") related to the NG technology. D.J.I. is a cofounder of Torque Therapeutics, which has licensed patents related to the NG platform. J.R.A., S.K.E., and D.J.I. are inventors on U.S. provisional patent no. 62/887,805 ("Engineering Regulatory T Cells with TCR-Signaling-Responsive IL-2 Nanogels and Methods of Use") related to the IL-2 NGs and methods thereof for improving T_{reg} therapy described in this manuscript. All other authors declare that they have no competing interests. **Data and materials availability:** All data associated with this study are present in the paper or the Supplementary Materials.

Submitted 4 June 2019
Resubmitted 3 June 2020
Accepted 3 September 2020
Published 11 November 2020
10.1126/scitranslmed.aaw4744

Citation: S. K. Eskandari, I. Sulkaj, M. B. Melo, N. Li, H. Allos, J. B. Alhaddad, B. Kollar, T. J. Borges, A. S. Eskandari, M. A. Zinter, S. Cai, J. P. Assaker, J. Y. Choi, B. S. Al Dulaijan, A. Mansouri, Y. Haik, B. A. Tannous, W. J. van Son, H. G. D. Leuvenink, B. Pomahac, L. V. Riella, L. Tang, M. A. J. Seelen, D. J. Irvine, J. R. Azzi, Regulatory T cells engineered with TCR signaling–responsive IL-2 nanogels suppress alloimmunity in sites of antigen encounter. *Sci. Transl. Med.* **12**, eaaw4744 (2020).

Science Translational Medicine

Regulatory T cells engineered with TCR signaling–responsive IL-2 nanogels suppress alloimmunity in sites of antigen encounter

Siawosh K. Eskandari, Ina Sulkaj, Mariane B. Melo, Na Li, Hazim Allos, Juliano B. Alhaddad, Branislav Kollar, Thiago J. Borges, Arach S. Eskandari, Max A. Zinter, Songjie Cai, Jean Pierre Assaker, John Y. Choi, Basmah S. Al Dulaijan, Amr Mansouri, Yousef Haik, Bakhos A. Tannous, Willem J. van Son, Henri G. D. Leuvenink, Bohdan Pomahac, Leonardo V. Riella, Li Tang, Marc A. J. Seelen, Darrell J. Irvine and Jamil R. Azzi

Sci Transl Med **12**, eaaw4744.
DOI: 10.1126/scitranslmed.aaw4744

Bring your own cytokine

T regulatory cells are a key part of the immune system, where they help suppress undesirable immune responses. Their potential therapeutic uses include various conditions caused by excessive or undesirable T cell activation, such as autoimmune disorders, graft-versus-host disease, and transplant rejection. To help maintain the activity of therapeutic T regulatory cells without concurrent activation of cytotoxic immune responses, Eskandari *et al* . equipped T regulatory cells with nanogel "backpacks" containing interleukin-2, engineered to release the cytokine under the appropriate conditions. The authors tested this approach in both murine and humanized models of skin transplantation, demonstrating the backpacked cells' effectiveness at suppressing alloimmunity.